

UNIVERSITÀ DELLA CALABRIA



UNIVERSITA' DELLA CALABRIA

Dipartimento di Fisica

Dottorato di Ricerca in

Scienze e Tecnologie Fisiche, Chimiche e dei Materiali
in convenzione con il CNR

CICLO

XXIX

**Realization of liquid crystalline composite structures organized
in non-cartesian orientations and their application in Photonics**

Settore Scientifico Disciplinare FIS/03

Coordinatore: Ch.mo Prof. Vincenzo Carbone

Firma Vincenzo Carbone

Supervisore/Tutor: Ch.mo Dr. Roberto Caputo

Firma Roberto Caputo

Dottorando: Domenico Alj

Firma Domenico Alj

Introduzione

In questo lavoro verranno esposte le attività salienti che hanno caratterizzato l'attività di ricerca durante il periodo di dottorato. In linea con la prevalente attività svolta nel laboratorio in cui è stato speso il maggior tempo di questo ciclo di dottorato, la tematica è stata fortemente correlata all'Ottica. La ricerca ha visto continuare lo studio sulla tecnica POLICRYPS che, nell'ultimo decennio, ha coinvolto ampie risorse del laboratorio. Questa tecnica ha permesso di produrre reticoli di diffrazione, a materiale composito (polimero-cristallo liquido) che, con eccezionali proprietà, hanno trovato spazio in studi pubblicati su numerose riviste scientifiche. L'implementazione di questa tecnica, che interesserà larga parte di questo lavoro, ha riguardato la realizzazione di reticoli circolari. Partendo dai reticoli circolari, nel presente lavoro, verranno proposte tecniche e materiali utili per realizzare dispositivi a simmetria circolare adatti ad applicazioni in ottica. Nel capitolo primo, attingendo alla letteratura scientifica, verranno esposte alcune delle tecniche più utilizzate per ottenere simmetrie circolari nella realizzazione di dispositivi ottici. In particolare, verrà discusso l'allineamento di cristalli liquidi e le tecniche descritte a tale scopo spazieranno dal più classico rubbing, fino al più moderno impiego di materiali fotoallineanti. Questi ultimi materiali, per la grande versatilità sperimentale che manifestano, saranno indicati come uno dei campi di pubblicazione più vivaci in cui si muoveranno i futuri lavori di ricerca. Sempre nel primo capitolo verrà poi introdotta la tecnica POLICRYPS ed una nuova classe di materiali con grandi potenzialità ed interessanti applicazioni in Ottica, i Nanocristalli di Cellulosa. Dalla precedente veloce introduzione, nel secondo capitolo, la tecnica POLICRYPS verrà più approfonditamente descritta. Questa descrizione riguarderà i materiali e la procedura sperimentale con la quale i reticoli di diffrazione sono stati storicamente prodotti. Troveranno spazio considerazioni sulla particolare disposizione raggiunta (ortogonale ai muri di polimero) dal Cristallo Liquido e sulle eccellenti proprietà dei POLICRYPS come reticoli di diffrazione. Nonostante ciò, il capitolo non sarà esaustivo sui numerosi impieghi che i POLICRYPS hanno avuto nell'ultimo decennio e sulla letteratura scientifica che hanno permesso di produrre. Il capitolo terzo descriverà i polar POLICRYPS, ovvero i reticoli a simmetria circolare ottenuti con questa tecnica. Il contenuto sarà ispirato dalla pubblicazione che ha seguito il periodo di sviluppo (D. Alj, R. Caputo, and C. Umeton, Opt. Lett. 39, 6201-6204 (2014)) e conterrà, con la descrizione del setup utilizzato, i risultati ottenuti. Sarà sottolineata la caratteristica orientazione assunta dal Cristallo Liquido fra i muri di polimero che, in questo caso, ri-

manendo ortogonale ai muri di polimero, sarà radiale. Non mancheranno di essere velocemente analizzate anche le problematiche e le limitazioni riscontrate durante la realizzazione. Il capitolo quattro esporrà l'applicazione che questi reticoli circolari hanno permesso nella generazione di Cylindrical Vector Beam. Il capitolo sarà impostato sulla pubblicazione che è seguita al periodo alla Bilkent University (Ankara, Turchia) nel gruppo del prof. G.Volpe. (D.Alj,S.Paladugu,R.Caputo,G.Volpe and C.Umeton, Appl. Phys. Lett. 107, 201101 (2016)). Saranno descritte alcune tecniche presenti in letteratura nella realizzazione di fasci con polarizzazione a simmetria cilindrica, appunto, Cylindrical Vector Beam, e verrà analizzato in quale modo possa aggiungersi a queste tecniche anche l'utilizzo di un polar POLICRYPS (anche chiamato polshape). Una cospicua parte del capitolo sarà dedicata all'analisi della polarizzazione in uscita attraverso la misura e l'analisi dei parametri di Stokes del sistema. Anche in questo caso verranno discusse alcune criticità dell'esperimento e le prospettive verso le quali possono essere indirizzati ulteriori studi. L'ultimo capitolo, il capitolo quinto, proporrà invece una nuova classe di materiali con potenziali applicazioni in Ottica, i Nanocristalli di Cellulosa. La produzione scientifica alla quale questo capitolo attinge per esporre le interessantissime proprietà di questi materiali è ampia, ed è prevalentemente rivolta alla analisi delle loro proprietà. Il capitolo si ispira al periodo trascorso all'Université du Luxembourg (Lussemburgo) nel gruppo del prof J.P.F. Lagerwall, durante il quale è stato possibile condurre alcuni esperimenti. Una delle sfide che coinvolge molteplici gruppi di lavoro sui Nanocristalli di Cellulosa, riguarda la possibilità di influenzare il loro orientamento ed in questa direzione sono state condotte alcune prove con il cui commento si concluderà il capitolo. Le conclusioni, quindi, faranno il punto su ogni parte del lavoro proposto proponendo spunti critici e suggerendo la direzione da percorrere in futuri studi.

Univerità della Calabria

Abstract

Dottorato

Scienze e Tecnologie Fisiche, Chimiche e dei Materiali

—

Realization of liquid crystalline composite structures organized in non-cartesian orientations and their application in Photonics

by Domenico ALJ

In this work a description of the main research activity performed during the last three years of PhD is reported. The macro argument treated is related with the functionalities of innovative materials with application in Optics. A special mention will be devoted to the circular symmetry and how to achieve it. To this regard, several techniques will be considered for influencing the organization and alignment of active optical materials like Liquid Crystals. In the following, this research activity will be critically analyzed in relation with similar results already reported in literature. These techniques span from the most classical "rubbing" technique to the most recent advancements provided by innovative photoaligned systems. A large part of this work will discuss the POLICRYPS technique, commonly involved in the realization of tunable diffractive structures, and its new application with circular gratings showing radial disposition of LCs. Through a Stokes parameters analysis, it will be demonstrated how these gratings, can be efficiently used to generate Cylindrical Vector Beams (CVBs). At the end, an overview will be proposed of the innovative application that the cellulose nanocrystals can find in optics. Brief comments on the preliminary test performed with this material will be also discussed.

Contents

Abstract	1
1 Circular Symmetry	5
1.1 Circular symmetry perspective	5
1.2 Photoalignment materials	7
1.3 q-plates	9
1.4 Policryps	10
1.5 Cellulose Nano-Crystals	11
1.6 Summary	11
2 Policryps	15
2.1 Polymer and Liquid Crystals, from PDLC to POLICRYPS	15
2.2 Fabrication	17
2.3 The mixture	19
2.4 Procedure	20
2.5 Results	21
3 From Cartesian to polar POLICRYPS geometry	24
3.1 Polar structures	24
3.2 Samples preparation and results	26
3.3 Conclusions	30
4 Polar POLICRYPS and CVB	33
4.1 Introduction	33
4.2 Polar POLICRYPS as CVB generator	35
4.3 Conclusions	39
5 Cellulose Nanocrystals (CNCs)	43
5.1 summary	43
5.2 Introduction to CNCs	43
5.3 CNC suspension, fingerprint and chiral-nematic phase	44
5.4 Pitch of the CNC helices and their orientation	45
5.5 CNCs alignment tests through template molding	48
5.6 Drying experiments	49
5.7 Conclusions	51
A Recording Policryps Structures in photonic crystal fiber	54
A.1 introduction	54
A.2 Methodology	55
A.3 Results	55

List of Figures

1.1	Circular Symmetry Examples	6
2.1	Typical morphology of a POLICRYPS grating	17
2.2	Sketch of POLICRYPS gratings production cycle	18
2.3	Diffusion process	19
2.4	Policryps-pdlc diffraction efficiency	21
3.1	Optical setup for the visible curing of polar POLICRYPS	25
3.2	Micrographs of a large area of sample	26
3.3	Micrographs of samples	26
3.4	Sketch of the diffraction pattern	28
4.1	HGorder	34
4.2	Micrographs of samples	35
4.3	Experimental setup	36
4.4	CVB polarizations shapes	38
4.5	Beam propagation	39
5.1	Cellulose cells and nanofibrils	43
5.2	CNC texture after drying	44
5.3	Helix sketch	45
5.4	Ligth reflecion	46
5.5	Sketches of template replica	47
5.6	Drying on templates	48
5.7	Drying experiments	49
5.8	Reported drying experiment	49
A.1	PCFs employed in the experiments.	54
A.2	PCFs recorded in the experiments.	55

To my Family

Chapter 1

Circular Symmetry

summary

- Circular symmetry prospective
- Photoalignment material
- q-plates
- Policryps
- Cellulose Nano-Crystals

NOTE: The following work will often deal with circular symmetry and circular/radial alignment. The first one is referred to all kind of symmetries that can be easily described by polar coordinates. The seconds one stresses, instead, the spatial distribution and molecular organization shown by a material.

1.1 Circular symmetry prospective

Circular symmetry is one of the most recurring symmetries in Nature. From the shape of cells to petals of flowers, a circular symmetry distribution often appears as the most promising way to favour evolution. In the animal (human included) kingdom, the common denominator of almost every vision apparatus is a circular symmetry. Any vision organ shows a circular (or eventually ellipsoidal) shape because other symmetries would be useless and uneasy. Mimicking Nature, technology requires this kind of symmetry in optics for almost every application related to imaging (cameras, magnifying systems, etc.). As such, researchers developing optical instruments cannot neglect this aspect in their work. However, even if this kind of symmetry is fundamental in many aspects of our life, when considering its merging with optics, several problems can arise. One of them is related to the very small scale of visible wavelengths (400-700nm) which reflects in

the techniques involved for the realization of micro/nano circular structures. When aiming at systems exploiting peculiar functions in optics, it is often necessary to produce details that are spatially comparable with visible wavelengths. A possibility to limit this difficulty is to apply Micro and Nano fabrication/techniques to the realization of 2D optical devices. That said, any material characterized by optical properties possibly showing circular symmetry (induced or not) might be extremely attractive for researchers and for potential industrial applications. In the field of Optics, there are many basic requirements that a material must fulfil to be considered useful. From the immediately understandable characteristic of transparency, to more exotic ones like birefringence or non-linear responses, all features are related to specific applications and utilized wavelengths. As an example, an optical device made for working with non-visible wavelengths, like infrared or ultraviolet, can look quite strange. One of the most studied and yet used materials for novel applications in Optics and Photonics are Liquid Crystals (LCs). From the middle of the last century, these chemical compounds have been massively studied by scientists to understand their properties and master their utilization in common use devices (displays). A fundamental requirement for LCs to be utilized, is their alignment on whatever substrate. Indeed, Nematics, the simplest kind of LCs, are cigar-shaped molecules that can show medium to long-range organization. The simplest organization is a unidirectional alignment, that can be induced by means of a mechanical rubbing. In more detail, for performing a rubbing a cloth is rubbed, always in the same direction, on a polymeric material (e.g. Polyimide) coated on the substrate where the alignment is to be realized. This rubbing creates micro-scale scratches on the polymer film that will successively align the LCs molecules. However, for the aforementioned applications, the idea to obtain a circular symmetry in the LCs molecular orientation was always sought for but difficult to obtain. For this reason, the first focus of research was on LCs systems with purely cartesian alignments (homeotropic, planar or mixed configurations). These studies resulted in a comprehensive insight of the behaviour of LCs when external stimuli (electric field or temperature) are applied. Recently, a new paradigm in research is emerging for realizing more complex functionalities in Optics. In more detail, the idea is to realize a LCs alignment that is spatially dependent. The first way to proceed in this direction is to achieve a non-cartesian or circular alignment. This approach can result in devices like tunable lenses or q-plates [1, 2] that are peculiar devices that can actively modify the polarization state of the incoming light and generate, for

instance, Cylindrical Vector Beams (CVBs)[3].

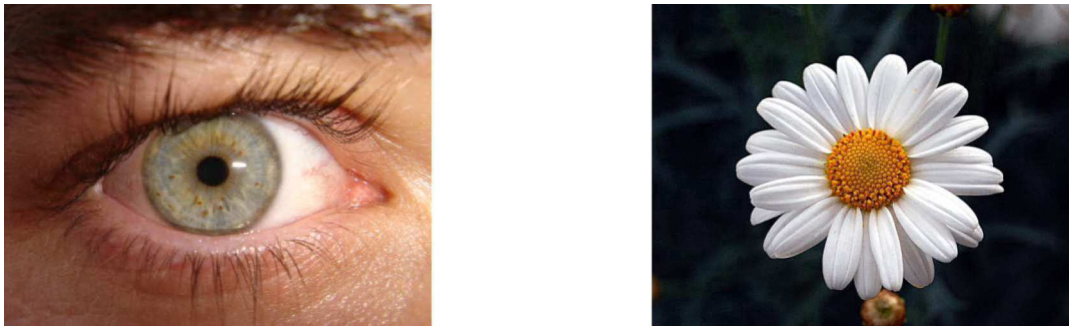


FIGURE 1.1: Circular Symmetries examples

1.2 Photoalignment materials

While the degree of freedom of mechanical rubbing techniques is limited to simple geometries, new intriguing possibilities appear when the alignment of LCs is provided by photo-alignment materials. These materials realize a proficient alignment layer for LCs that can be managed and directed by exploiting the state of polarization of light. The combination of this features with masks, polarizers or digital systems for polarization control allows a variety of possible geometries. A given pattern, generated with polarized light, can be replicated on a thin layer of photo-alignment material, previously spin-coated on a surface [4, 5]. The polarization pattern can be obtained for example by using a Spatial Light Modulator (SLM), an interference pattern or holography in general, with a resolution that can be pushed to the nanometric scale. Then, LCs will be layered on the surface treated with the photo-alignment material and they will assume its same alignment. By using this technique, it is even possible to reproduce images in the LCs [4, 5]. The photo-alignment material is made of polarization sensitive molecules that can be optically oriented throughout a defined range of wavelengths and intensities. Their intrinsic birefringence is small, thus not affecting the one of the materials to be aligned. To safeguard the robustness and durability of eventual devices, molecules chemical engineering is usually performed to maximize the wavelength sensitivity in the UV range that is usually well far from operative ranges. This allows to realize extraordinary conditions never

achieved before or highly difficult to achieve with standard mechanical alignment means. Research in photo-alignment materials is very active and in literature many works can be found dealing with possible applications [4, 5]. The efficient polarization control holds the promise of exploiting effects and phenomena that can expand the functionalities and enhance the capabilities of optical systems. In fact, this is the core of Tabiryan's idea [6, 7] for optics of the 4th generation, following optics based on simple shape (1st generation), refractive index (2nd generation), and effective birefringence (3rd generation). Recent publications have shown how photo-alignment overcame the rubbing technique in the realization of circular symmetries. Thus, new kind of devices, q-plates like [2], were recently realized using photo-alignment in combination with Cholesteric Liquid Crystals (CLCs) in order to realize a Bragg-Berry mirror [8]. CLCs are peculiar kinds of LCs that show a stack of nematics layers whose average in-plane molecular orientation is rotated of a given angle while moving along the vertical direction. This gives rise to a helical organization of the material. The device realized in [8] comprises a more complex CLCs geometry where the initial orientation of CLCs helices has a radial symmetry. This was possible thanks to the features of the photo alignment used that immobilized the nematic molecules of the initial helix layer in a radial distribution on the surface. This distribution was non achievable with standard rubbing technique because in the best case, the distribution would have been not radial but circular induced by a rotation (in a chosen sense) of the plate containing the substrate and in contact with the rubbing cloth. One of the most useful applications of photo alignment materials is related to digital polarization holography [7]. This technique exploits a device (Spatial Light Modulator, SLM) that is able to modulate amplitude, phase or polarization of light waves in space and time to generate custom arbitrary patterns. By combining the functionalities of photo alignment materials with the use of an SLM, it is virtually possible to produce any desired geometry. The process is straightforward. The SLM illuminates the photoalignment layer with the spatially dependent polarization geometry. The orientation of the molecules constituting the layer is modified accordingly. Once a birefringent material (LCs) is put in contact with the photo-alignment layer, the spatially dependent alignment will be transferred to it and the resulting geometry will be visible between crossed polarizers.

1.3 q-plates

A monochromatic light beam traveling along a given axis z , can transport angular momentum, oriented as the propagation direction, in two different form [2, 9, 10, 11]. This two forms are a classical part associated with circular polarization (also referred as SAM, Spin Angular Momentum) and the second, named “orbital”, associated with the phase profile (also called OAM, Orbital Angular Momentum). Following what has been proposed in literature [2], a device able to convert SAM into OAM, is called q-plate. They are introduced as a device “made as a birefringent liquid crystal plate having an azimuthal distribution of the local optical axis in the transverse plane, with a topological charge q at its center defect.” Throughout q-plates many works have been done in optical trapping and cylindrical vector beam (CVB) generation. This two field are strongly related and often they are each other complementary in applications. What the photo alignment material can provides is the possibility to realize q-plate with broad degree of freedom in geometry. All different geometries of q-plates [12] and non symmetric structures, can be easily reached due the capability to replicate a polarization pattern on the photo alignment material. This was impossible or very difficult until their development because the way to realize q-plates was delegate to micro-nanofabrications [13]. The main problem occurring when light properties need to be modified, is intertwined with the scale on which we must push our fabrications. In this sense, new lands have been explored from recent years with new technology in nano fabrication, that allowed researchers to realize high precision structures close to few nano-meter level. A key parameter to manipulate the characteristic of a phenomenon as light, in the scale of hundred nanometer, is the sub hundred nanometer dimension of the structure with which the light interacts. As technology teaches from the ancient time, what is possible now, is the effect of multiples developments in many fields. In the case of nano fabrication, the developments required, spread in many fields, electronics, computer software, lasers, materials. One of the most exciting instruments that appears in the last decades and which attract a lot of interest from sciences research, is for example, Nanoscribe®. It is largely used for multiple purposes in research. The applications that Nanoscribe® helps to realize covers a large area of experimental science, from biology to optics and microfluidic. To see better on the evolution in fabrication of q-plates, two examples taken by literature can be used. Ten

years ago, an interesting articles was published on the field of Pancharatnam phase studies through the employment of a q-plate [14]. The q-plate used, with the rubbing technique above described, was a device working on the field of Pancharatnam-Berry phase, which is, as reported in literature “a geometric phase associated with the polarization of light. When the polarization of a beam traverses a closed loop on the Poincaré sphere, the final state differs from the initial state by a phase factor equal to half of the Ω area, encompassed by the loop on the sphere.[15, 16, 17] ” . The optical active material used [14] was a Nematic Liquid Crystal (E63) that, due rubbing, self disposed along the circular line of rubbing. In this way, researches demonstrated the possibility to realize a cheap device, in the visible domain, able to generate switchable helical modes. After ten years, in the same field, with a similar device but a different interest, another articles have been published. In this case, indeed, the alignment layer was realized by the employment of a photo alignment[8]. The freedom to dispose in a circular or radial ways the photo alignment molecules, allowed researchers to introduce a new degree of freedom in the disposition of a cholesteric liquid crystal (MDA-02-3211) used in this work. Through a radial disposition of photo alignment the disposition of helical structures followed this symmetry on the two interfaces of a cells.

Many efforts have been spent in the improvement of macro optical devices with active material or without. This has been going to open every day more, a new frontier of optics that, from decades, is investigated with interest. Researchers are probably close to new developments that will modify again our vision of the possibilities of optics.

1.4 Policryps

The possibility to obtain an alignment of LCs can be reached not only with the employment of an alignment layer. POLICRYPS (Polymer Liquid Crystals Polymer Slice) allowed to realize a linear disposition of liquid crystals between polymeric walls without any alignment materials [18]. This disposition, in combination with the possibilities, to switch the orientation of LC allowed to realize gratings with a special features of tunability. During the realization, no alignment substrate or other dopant agent is required to achieve alignment of LCs. In this case the alignment is provided by the chemical diffusion force during the fabrication. This technique involve simple materials

and focus high attention in the procedure of fabrication that stress the fundamental role of other parameters. Polymerization induced by an interferometric pattern is the keyword of POLICRYPS technique. This is connected with a non interacting element as LCs during polymerization that easily diffuse in the low intensity regions of the pattern by the isotropic phase they have during illumination. In this way is possible to achieve a linear disposition of LCs between the polymeric walls and, as a result from the interference of two lasers beams, a 1D polymeric structure, as gratings. The alignment can be reached also when a pattern of concentrically rings is used instead a slices one. In this case, what happen is the radial alignment between the walls of the concentric circles of pattern and what result from, is a circular grating [19]. (both techniques and structures will be treated in the following chapters)

1.5 Cellulose Nano-Crystals

Under certain conditions and for some special materials, alignment can be spontaneous. It is the case of Self-Assembly materials as the Cellulose Nano-Crystals (CNCs) are. CNCs are rods shape natural derived material with extremely intriguing characteristic. Research on that materials involved a lot of groups [20, 21, 22, 23, 24] for possible applications in many fields. The big challenges is still to achieve a optimal control of their self assembly behavior in a specific order. Typically CNCs are stored in water suspension in a small concentration. Their special characteristic of birefringence in combination with a liquid crystalline state, attract the scientific interest in optic. Generally, a way to study their disposition, involve the drying of suspension and AFM/SEM studies. Through the symmetry of forces in a drop formation, it is possible to observe a symmetric disposition of material after the drying of suspension. Applications of CNCs in optics and photonics are still at the beginning state, but research can provide in few time, with an ultimate effort, new results (more about CNC in the following chapters).

1.6 Summarize

All above shown examples of how it is possible to obtain circular symmetry of optical material. All possible application are still investigated and many

works are continuously published. Many of literature show how is possible to obtain high order laser beam and cylindrical vector beam (CVB). The applications involving CVB are focused mainly on optical trapping. Studies are also performed in the field of quantum information using the special features that a CVB can carry out (e.g.[25]). For applications, a growing interested is largely devoted to Bio-compatible and Natural-derived materials. Extremely new and intriguing studies are investigating human applications for correction of eyes defects. This activity involves public and private researchers and is possible to suppose to see in short time, new incredible applications.

Bibliography

- [1] O. Pishnyak, S. Sato, and O. Lavrentovich, *Appl. Opt.* 45, 4576-4582 (2006).
- [2] L. Marrucci, C. Manzo, and D. Paparo, *Phys. Rev. Lett.* 96,163905 (2006).
- [3] Q. Zhan, *Adv. Opt. Photonics* 1, 1 (2009).
- [4] L. De Sio, D. Roberts, Z. Liao, S. Nersisyan, O. Uskova, L. Wickboldt, N. Tabirian, D. Steeves, and B. Kimball, *Opt. Express* 24, 18297-18306 (2016).
- [5] J.Kobashi,H.Yoshida& M. Ozaki. *Nature Photonics* 10,389392 (2016)
- [6] N. Tabirian, in 11th Workshop, Novel Optical Materials and Applications (Cetraro, Italy, 2013).
- [7] L. De Sio,D.E. Roberts, N.V. Tabirian,D.M. Steeves,B.R. Kimball; (Conference Presentation). *Proc. SPIE* 9940, *Liquid Crystals XX*, 994007 (November 3, 2016);
- [8] M. Rafayelyan and E. Brasselet, *Opt. Lett.* 41, 3972-3975 (2016).
- [9] J. Humblet, *Physica (Amsterdam)* 10, 585 (1943)
- [10] G. Abbate, P. Maddalena, L. Marrucci, L. Saetta, and E. Santamato, *Phys. Scr.* T39, 389 (1991).
- [11] L. Allen, M. W. Beijersbergen, R. J. C. Spreeuw, and J. P. Woerdman, *Phys. Rev. A* 45, 8185 (1992).
- [12] L.Marrucci,E.Karimi,S.Slussarenko,B.Piccirillo,E.Santamato,E.Nagali and F.Sciarrino *J.Opt.*13(2011)
- [13] E.Brasselet, M.malinauskas,A.Žukauskas and S.Juodkazis. *Appl.Phys.Lett.* 97,211108 (2016)
- [14] L.Marrucci,C.Manzo and D.Paparo *Appl.Phys.Lett* 88,221102 (2016)

- [15] Z. Bomzon, G. Biener, V. Kleiner, and E. Hasman, *Opt. Lett.* 27, 1141-1143 (2002).
- [16] S. Pancharatnam, *Proc. Indian Acad. Sci. Sect. A* 44,247 (1956)
- [17] M. V. Berry, *Proc. R. Soc. London Ser. A* 392, 45 (1984).
- [18] Caputo, R.; DeLuca, A.; DeSio, L.; Pezzi, L.; Strangi, G.; Umeton, C.; Veltri, A.; Asquini, R.; d'Alessandro, A.; Donisi, D.; Beccherelli, R.; Sukhov, A. V.; Tabiryan, N. V. *Journal of Optics A: Pure and Applied Optics*, Volume 11, Issue 2, article id. 024017, 13 pp. (2009).
- [19] D. Alj, R. Caputo, and C. Umeton, *Opt. Lett.* 39, 6201-6204 (2014).
- [20] Fratzl, P. Biomimetic materials research: what can we really learn from nature's structural materials *J. R. Soc. Interface* 4, 637642 (2007).
- [21] Klemm, D., Kramer, F., Moritz, S., Lindstrom, T., Ankerfors, M., Gray, D. & Dorris, A. Nanocelluloses: a new family of nature-based materials. *Angew. Chem. Int. Edit.* 50,54385466 (2011).
- [22] Habibi, Y., Lucia, L. & Rojas, O. J. Cellulose nanocrystals: chemistry, self-assembly, and applications. *Chem. Rev.* 110, 34793500 (2010)
- [23] J. P. F. Lagerwall, C. Schtz, M. Salajkova, J. Noh, J. H. Park, G. Scalia, L. Bergström, *NPG Asia Mater.* 2014, 6, e80.
- [24] Park, J. H., Noh, J., Schütz, C., Salazar-Alvarez, G., Scalia, G., Bergström, L. and Lagerwall, J. P. F. (2014), Macroscopic Control of Helix Orientation in Films Dried from Cholesteric Liquid-Crystalline Cellulose Nanocrystal Suspensions. *ChemPhysChem*, 15: 14771484. doi:10.1002/cphc.201400062
- [25] Parigi, V. et al. Storage and retrieval of vector beams of light in a multiple-degree-of-freedom quantum memory. *Nat. Commun.* 6:7706 doi: 10.1038/ncomms8706 (2015).

Chapter 2

Policryps

summary

- Polimer and Liquid Crystals, From PDLC to POLICRYPS
- Fabrication
- The mixture
- Procedure
- Results

2.1 Polymer and Liquid Crystals, from PDLC to POLICRYPS

Since the end of 80s, a growing interest from researchers was oriented to the study and realization of composite devices made of polymer and liquid crystals. In particular, the possibility to control, by means of external fields (electric, magnetic or temperature variation) the orientation and characteristics of LCs in a polymer matrix, was intended as an optimal way for realizing novel and intriguing applications. On this way, the first works employed LCs dispersed into a polymeric matrix and were thus called PDLCs (Polymer-Dispersed Liquid Crystals) [1, 2]. In this early device, by means of a photo-polymerization process, a polymeric matrix trapped LCs in droplets with different sizes ranging from few hundreds of nanometers to several microns. The optical behaviour of the device was strongly dependent on the droplet size. Investigations have been performed and, as it is easy to understand, large differences have been observed. Indeed, the scattering of

light drastically changes in dependence of the droplet size and the properties of the device are consequently strongly modified. The first works of Margerum[1] and Sutherland[2, 3], performed during the beginning of 90s, demonstrated that, from a homogeneous polymerization of a mixture comprising pre-polymer and LCs, a simple device could be obtained whose transparency was controlled at will by simple application of an external electric field. Following these first attempts, an intense study started for the realization of switchable diffraction gratings based on a similar principle [4]. Both theoretically and experimentally, the researchers have been involved in the realization and improvement of this device. For what concerns theory, they studied what are the main parameters influencing the diffusion of LCs and their phase-separation from the polymer component during the photopolymerization process. The interest was in understanding how this could be controlled and eventually maximized. On the experimental side, the effort was mainly spent on improving the structure morphology and the switching performance. For fabricating the device, a two-beams holographic pattern was used and the obtained diffracting structure was called H-PDLC from the shortening of holographic PDLCs. In this case, LCs in the grating needed a relatively low electric field to switch, but the scattering losses, due to the big size of droplets limited the possible applications. Accurate studies revealed that the presence of LC droplets was due to the low diffusion of LCs that are required to migrate from the bright areas of the interference pattern, where polymerization grows rapidly, to the low-intensity ones, where polymerization is almost absent. Once this issue was identified, researchers combined experimental and theoretical knowledge to obtain an optimal phase separation between polymers and LCs. As such, the natural evolution in research of H-PDLCs, with high phase separation between polymer and LCs, with no droplets and relatively low switching voltage of LCs, has been the POLICRYPS paradigm. As mentioned above, this acronym stands for Polymer Lyquid Crystals Polymer Slices and resumes the main characteristic of these gratings. Indeed, the result is a periodic repetition of polymer and LCs with an almost perfect phase separation, thus no droplets. The absence of nematic liquid crystals (NLCs) droplets is related to the higher mobility, possessed by NLC molecules, when the material is in isotropic phase with respect to the one the molecules have in the nematic phase. The solution to the droplets issue was brought by temperature, which resulted in an innovative technique called MPTIPS (Mixed Polymerisation Thermal Induced

Phase Separation). Following this technique, the fabrication procedure follows three main steps[4-8]:

- a) To avoid the presence of a nematic phase during the curing process, the mixture of monomer (with its photoinitiator) and NLCs is heated until the isotropic phase of that;
- b) the sample is illuminated with the UV laser pattern to start the polymerisation;
- c) after curing, the sample is slowly cooled to nematic phase of NLCs (typically it is cooled to room temperature). This process is a key point and the slow cooling is a key parameter to reach a good disposition of liquid crystals.

The well defined repetition of polymer and NLC show, in a POLICRYPS morphology (Figure 2.1), an excellent alignment of LCs between polymeric walls. The orientation of the LCs molecular director was very much discussed. Several evidences brought to confirm that the orientation of the nematic molecular director is parallel to the sample slabs and perpendicular to the polymer walls inside the grating. A first but not sufficient observation in this sense has been seen by performing a polarized optical microscope (POM) observation. A POLICRYPS shows a drastic increase of the transmittance when the wave-vector of the grating forms an angle of $\pi/4$ with the polarizer axis. Even if this confirms a good alignment between the polymeric walls, the discussion between homeotropic or planar orientation with respect the polymer slice could still be plausible. A proof is obtained by analysing the diffraction efficiency of the grating with s and p polarized probe beam. The difference between the two polarisations, stresses a much higher diffraction efficiency with p-polarized probe beam. It means that s-wave experiences the ordinary refractive index of the NLC which almost completely matches the index of the polymer. This qualitative result also confirms that, during the diffusion process, the NLC molecules align perpendicularly to the polymeric walls.

2.2 Fabrication

The idea at the basis of the POLICRYPS fabrication is to avoid, during polymerisation, the droplets formation and for this reason the NLC is maintained

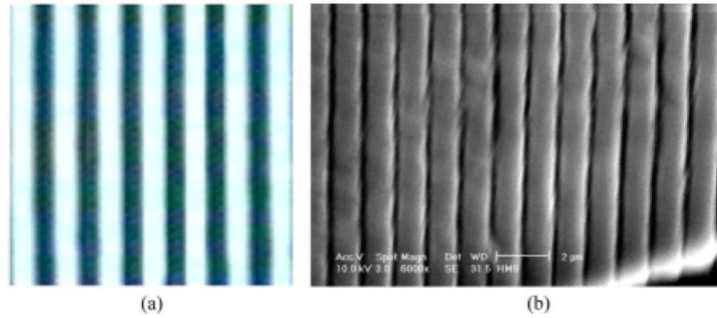


FIGURE 2.1: Typical morphology of a POLICRYPS grating; a) $\Lambda = 3.6\mu m$ image taken by POM; b) $\Lambda = 1.3\mu m$ image taken by Scanning Electron Microscope

(at high temperature) in isotropic phase. Photo polymerisation is the responsible of the diffusion of LCs from the creating polymer component. This diffusion is promoted by the conventional Fick diffusion due to the redistribution of molecules to equalize the chemical potentials of the involved chemical species. In order to model the system that leads to POLICRYPS, an important assumption is made in considering as immobile the long polymeric chains. In more detail, the growth in concentration of the polymer component in the high intensity regions of the curing interference pattern corresponds to a concentration decrease of the monomer component, hence diffusion of monomer from low intensity regions to high ones takes place. At the same time, the formation of polymer chains, which occupy most of the available volume in correspondance to the high intensity regions of the curing pattern, push the LC component away in the low intensity regions. This is consistent with the idea that the diffusion of LCs takes place preferably in the regions not occupied by non-reacting components. Even if this assumption tremendously simplifies the description of the problem, the system still remains highly non-linear. Historically, the fabrication of POLICRYPS have been employs an Ar-ion Laser source ($\lambda = 351\text{nm}$). The set-up is a very simple holographic arrangement comprising two beams, quite similar to a system for diffraction efficiency measurements. A laser beam is expanded and splitted into two equal intensity beams before being recombined again on the sample surface. In this geometry, it is easy to change the interference angle from few degrees up to 60° as such to influence the periodicity of the interference pattern and hence the pitch of the grating. A key point of the curing procedure is intertwined with the isotropic state of the monomer-LCs mixture. The control of the sample temperature is provided by a programmable

hot-stage where the curing sample can be heated, stabilized at a given temperature, and cooled to room temperature (Figure 2.2).

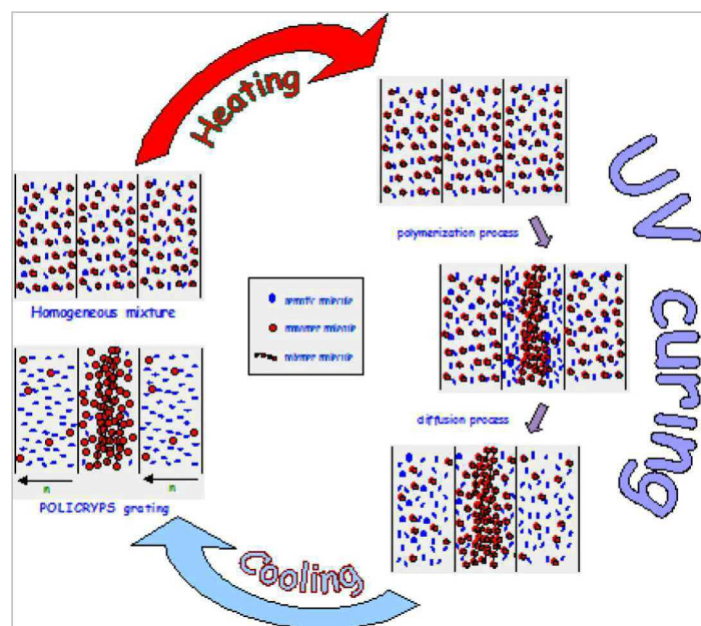


FIGURE 2.2: Sketch of POLICRYPS gratings production cycle.

2.3 The mixture

In research, it happens, not rarely, that a simple solution can lead to optimal results. In a certain way, this fits with the mixture chosen for the POLICRYPS fabrication. In case of H-PDLCs, skilled chemists developed from scratch a quite efficient mixture made of several components with ad-hoc functionalities to achieve the best result in terms of polymerization and re-distribution of LCs and polymer during curing. They ended up with a five components mixture that is quite complex to prepare. However, they did not consider the curing process in itself to improve the obtainable result. In case of POLICRYPS, it happened exactly the contrary. Instead of numerous components, just two materials have been mixed up and the simplification was possible because of a ready-to-use commercial UV polymerizable mixture produced by NORLAND Optics (NOA-61) that was combined with a usual, commercial and easy-to-find Liquid Crystal (5CB or E7). If the reliability of the commercial product concentration is considered high (as it is logical to suppose), the key parameter in the mixture, for being successful in POLICRYPS preparation is only the relative weight concentration of

NOA-61 and LCs. This relation has been empirically studied and reported and corresponds to a maximum concentration of LCs in the total amount of the mixture of about 27%-28 wt%. This is the best way for the resulting device to show an extremely good separation between polymer and LCs and no droplets are visible at the POM. Higher LCs concentration would result in spontaneous phase separation before curing.

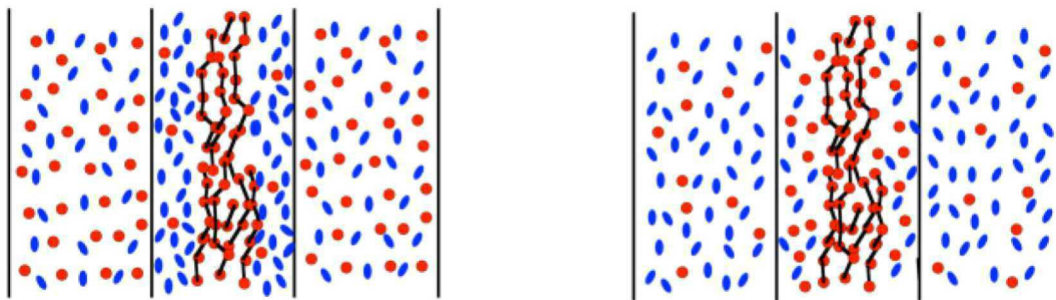


FIGURE 2.3: ■ nematic molecule; ● monomer molecule; —●— polymeric chain
Distribution of liquid crystal, monomer and polymer molecules. Monomer molecules are denoted by circles, nematic molecules by cylinders, polymer chains by interconnected circles

If a visible instead of a UV laser source is considered for curing, a convenient photoinitiator is to be included in the mixture. As it will be shown in the next chapter, by using an additional small percentage (ca 1 wt%) of a visible photoinitiator, it is possible obtain satisfactory results even curing with visible laser radiation. However, in this case, it has been observed that the separation of liquid crystals from polymer is not perfect, hence resulting in a not completely pure morphology.

2.4 Procedure

All fabrication of this kind of diffraction gratings starts from the careful preparation of cells, made of two glass substrates put at controlled distance, where the pre-polymer mixture will be infiltrated by capillarity and then cured. The typical thickness used is about 10 μ m and, to avoid optical defects, it requires much care as only fabrication in a controlled environment (clean room) typically allows. The cells are usually made with clean ITO-coated glasses that ensure electrical conductivity and allow the application of an externally applied electric field to the resulting structure. After filling the cell by capillarity

with the mixture of monomer and LC, it is placed in the hot stage where the incoming interference pattern will cure it. About that pattern, as mentioned, it is the result of the interference between two beams originating from the same source (AR-ion laser $\lambda = 351\text{nm}$). The stability of the beam has a strong influence in the final result. The total curing intensity, as sum of the two beam intensities has been empirically established and corresponds to few milliwatts per square centimeter. To guarantee an adequate fringe visibility and hence an optimal curing condition, the two arms of the setup can have at most a difference of about 10% in power. The typical time of curing in this condition is about 1000 sec in accordance with a slow and almost complete diffusion (Figure 2.3) of LCs from the region where the polymeric chain start growing.

2.5 The results

The idea that moves the research in POLICRYPS, is related with the possibility to achieve a switchable grating with a high diffraction efficiency, low scattering losses and low switching voltages. The morphology of the structures, with the long axis of the LC molecules oriented perpendicular to the polymeric walls, have inspired the researchers to find a LC whose ordinary refractive index matches the refractive index of the polymer. On this way, by assuming a complete reorientation of the LC component upon application of the external electric field, a completely commutable grating can be theoretically produced. However, it is to be considered that the diffracting performance of the grating is strongly dependent on the probing electric field polarization. In case an s-polarized field is considered (i.e. field parallel to the polymeric walls), the index matching gives rise to an almost absent diffraction grating (the index modulation along the grating is almost zero) that remains so also upon electric field application.

In the other case (p-polarized field, perpendicular to the polymeric walls), the extraordinary index of LC (5BC or E7), typically equal to about 1.72, is much different than the polymer index (1.54) thus the grating shows the highest diffraction efficiency in normal conditions and the grating disappears almost completely, when the electric field is applied. Typically, the diffraction efficiency is measured as the ratio of the first diffracted order intensity over the transmitted beam one. This can be very high (about 98% in Bragg configuration) in POLICRYPS and it is for sure one of the most interesting features of

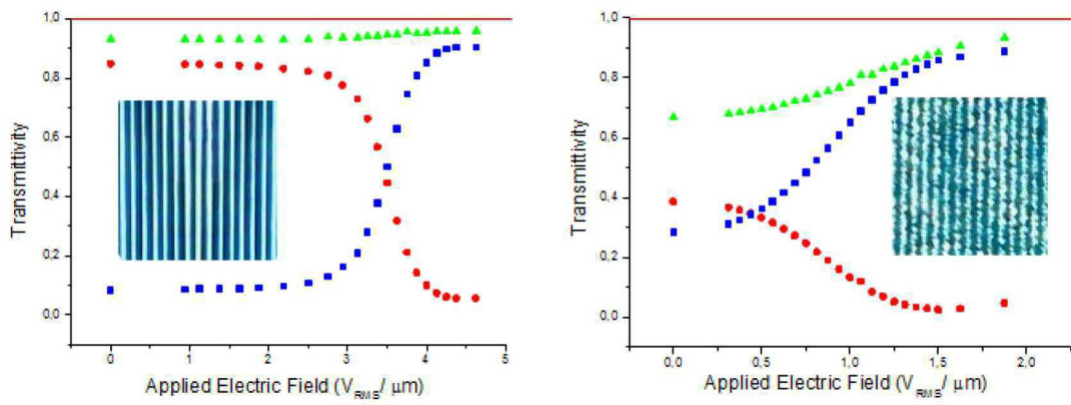


FIGURE 2.4: Electric field dependence of zeroth-order transmittivity T (squares), first-order transmittivity T (circles) and total transmittivity T (triangles) for: (left) POLICRYPS grating and (right) HPDLC grating at room temperature. Error bars are of the order of the dot size. The pictures in the boxes show, respectively, a typical POLICRYPS and HPDLC grating morphology with the same spatial period

those. What was measured as a switching electric field, was about $3\text{-}5\text{ V}/\mu\text{m}$ and it means about $30\text{-}50\text{ V}$ for a $10\mu\text{m}$ thick sample. The electric potential for switching is not as low as in case of a pure LC cell and this is probably related to the presence of polymeric chains in the LC areas. Still, this result is much better than the typical H-PDLCs performance (about $10\text{-}15\text{ V}/\mu\text{m}$) where the surface tension forces, related to the presence of LC droplets, severely degrade the device functionality. The mechanism that changes the orientation of LCs is obviously related to the Fredericks transition [6] that affects the liquid crystal molecules. The measurements shown in Figure 2.4 reveal how well, in a typical POLICRYPS structure, the first and the zero orders can be switched upon application of an external electric field.

Bibliography

- [1] Margerum J D, Lackner A M, Ramos E, Smith G W, Vaz N A, Kohler J L and Allison C R 1992 Polymer dispersed liquid crystal film devices US Patent Specification 5,096,282 (March 17)
- [2] Sutherland R L, Tondiglia V P, Natarajan L V, Bunning T J and Adams W W 1996 Electro-optical switching characteristics of volume holograms in polymer dispersed liquid crystals J. Nonlinear Opt. Phys. Mater. 5 8998
- [3] Sutherland R L, Tondiglia V P, Natarajan L V, Bunning T J and Adams W W 1994 Electrically switchable volume gratings in polymer-dispersed liquid crystals Appl. Phys. Lett. 64 10746
- [4] Caputo R, De Sio L, Sukhov A V, Veltri A and Umeton C 2004 Development of a new kind of switchable holographic grating made of liquid crystal films separated by slices of polymeric material (policryps) Opt. Lett. 29 1261
- [5] Caputo R, Sukhov A V, Tabyrian N V, Umeton C and Ushakov R F 2001 Mass transfer processes induced by inhomogeneous photopolymerisation in a multicomponent medium Chem. Phys. 271 32335
- [6] de Gennes P G 1993 The Physics of Liquid Crystals (Oxford:Clarendon)
- [7] P.S.Drzaich, Liquid Crystal Dispersions, World Scientific Publishers, Singapore, (1995).
- [8] Caputo R, Sukhov A V, Umeton C P and Ushakov R F 2000 Formation of a grating of submicron nematic layers by photopolymerization of nematic-containing mixtures J. Exp. Theor. Phys. 91 11907

Chapter 3

From Cartesian to polar POLICRYPS geometry

From

© Opt. Lett. 39, 6201-6204 (2014).

Part of the work herein reported is reprinted/adapted with permission,
from D. Alj, R. Caputo, and C. Umeton,

"From Cartesian to polar: a new POLICRYPS geometry for realizing circular
optical diffraction gratings,"

3.1 Polar structures

As described in the previous chapter, POLICRYPS technique allows to realize monodimensional gratings with a high quality morphology. The presence of composite materials as LCs and polymer, confers to these structures some special features. In past, with this technique, also two-dimensional gratings have been realized. In one of these realizations, a "two steps" POLICRYPS procedure was employed on the same sample. The first step was the realization of a monodimensional grating. After that, LCs contained in the sample were washed away by means of a solvent (tetrahydrofuran) in order to obtain an "empty grating". This empty structure was then involved as a template, re-filled with fresh LCs/pre-polymer syrup and cured again but in an orthogonal direction in such a way to result in a two dimensional geometry [1]. This has not been the only approach used for realizing two dimensional gratings. Another study has exploited a "one-step" procedure by using a Spatial Light Modulator (SLM) [2] by which a two-dimensional

pattern has been used to cure the sample. Both these studies realized what can be called a "Cartesian" morphology, i.e. a 2D square geometry sculptured in the photo-sensitive material. If the POLICRYPS procedure is applied by using a concentric curing pattern, it is possible to commute from the standard Cartesian geometry structure to a Polar one still keeping high-quality standards for the morphology. The interest of such a structure is at least two-fold. First of all, it behaves as a circular diffraction grating working in the visible range; to our knowledge, this is the first time that such a result is realized by exploiting holographic means. Second, the intrinsic LC director orientation exhibited in all the rings of the sample represents a promising opportunity for realizing optical q-plates and related applications. In our experiment [3], the pattern has been generated by a continuous-wave green laser source, (Verdi by Coherent, $\lambda = 532$ nm), and controlled, as usual, by a $\lambda/2$ plate and a polarizing beam-splitter. In order to generate a concentric circular pattern the beam is tightly focused by a microscope objective to an almost point source of coherent light that, imaged by the "recombination lens", experiences a spherical aberration. In the longitudinal spherical aberration (LSA) image-space of the lens, a centrosymmetric diffraction pattern is produced, whose center is located on the optical axis of the system (Figure 3.1, inset). The produced pattern consists of very closely spaced concentric rings with a typical spacing that can range from few to tens of micrometers, depending on the specific values of involved geometrical parameters. Due to spherical aberration, light rays coming from the lens L1 are not all focused in the same point; marginal rays (passing through the lens in its extreme outer parts) focus closest to the lens, while rays passing through the lens center focus at the most distant point from the lens. The region between these two focal points (Fig. 1, inset) is called LSA region. The presence of a ring pattern is understood by considering that, on a given plane perpendicular to the optical axis) in the LSA region, light beams come from different annular regions of the lens; therefore, depending on their different optical paths, beams have different converging wave-fronts, which may constructively or destructively interfere, thus producing bright and dark rings. A model, based on the diffraction theory of converging waves in presence of spherical aberration, allows to predict the pattern fringe spacing anywhere in the LSA region. The radial distance from the center of the pattern to the n th ring null point is calculated as $\rho_n = \beta_n z / ka$, where β_n is the n th root of the Bessel function $J_0(ka\rho_n/z)$ [3], k the wavevector of the impinging light, z the distance, along the optical axis, from lens L1 to the plane containing the considered ring pattern, and a is the

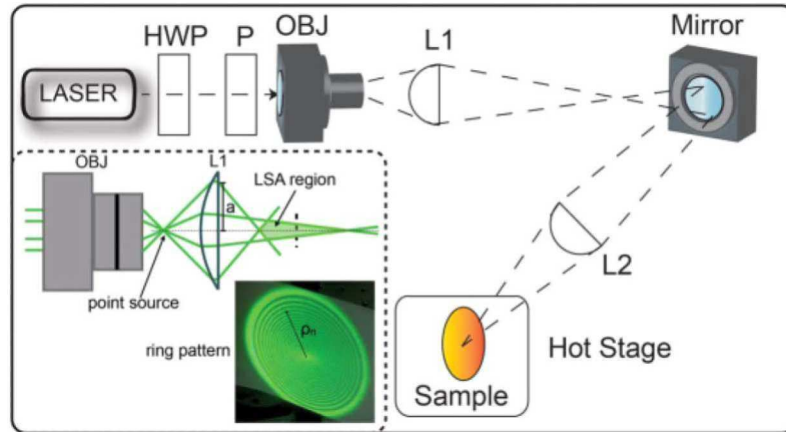


FIGURE 3.1: Optical setup for the visible curing of polar POLICRYPS optical diffraction gratings. Laser, CW solid-state laser; P, Polarizing beam splitter; HWP, $\lambda/2$ plate; OBJ, microscope objective (10X); L1, L2, spherical lenses. The sample is put in a hot-stage to control its temperature. In the inset: sketch of the spherical aberration the laser beam undergoes passing through the lens L1 and the ring pattern imaged on a plane perpendicular to the optical axis of the system.

radius of the illuminated circular area on the lens surface. The obtained pattern can be focused on the sample surface by another lens (L2), or can be used as it is by moving the sample. This ample flexibility in the choice of involved geometric parameters makes the proposed technique quite straightforward and easy to implement. Moreover, being the used elements easily available in every optics lab, the technique results also cost-effective.

3.2 Samples preparation and results

Samples are assembled as for a classical POLICRYPS by putting two glass substrates at a controlled distance ($10 \mu\text{m}$), to form a cell that is, later on, filled in by capillarity with a photosensitive syrup; this is made of the pre-polymer system NOA61 (70-72% wt, by Norland), the nematic liquid crystal (NLC) E7 (28-30% wt, by Merck) and for this case, an addition of the photo-initiator Irgacure 784 (1-2% wt, by BASF Resins). The choice of the mixture composition is the result of a study performed to extend the use of the POLICRYPS technology also to systems exploiting visible-light curing [2]. For the fabrication of all samples used in this kind of samples production, the standard

POLICRYPS protocol is followed (see Chapter 2) [4]. Micrographs of the obtained morphologies (taken between crossed polarizers at the polarized optical microscope, POM) are shown in Figure 3.2 and Figure 3.3

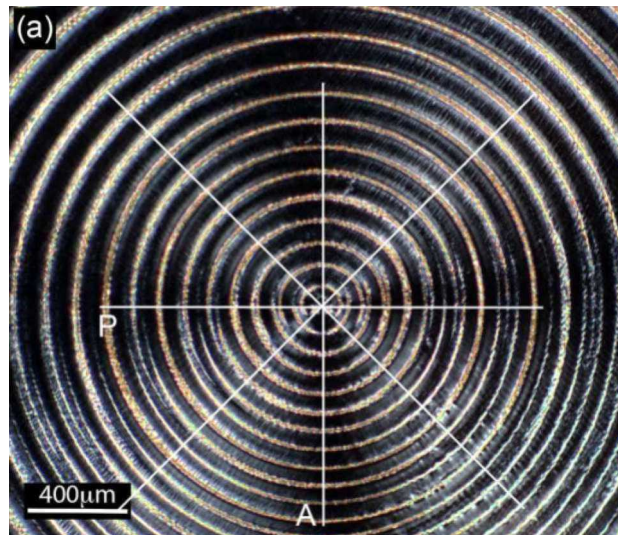


FIGURE 3.2: Micrographs (taken at the POM between crossed polarizers) of the morphology on large area obtained by exploiting the optical setup

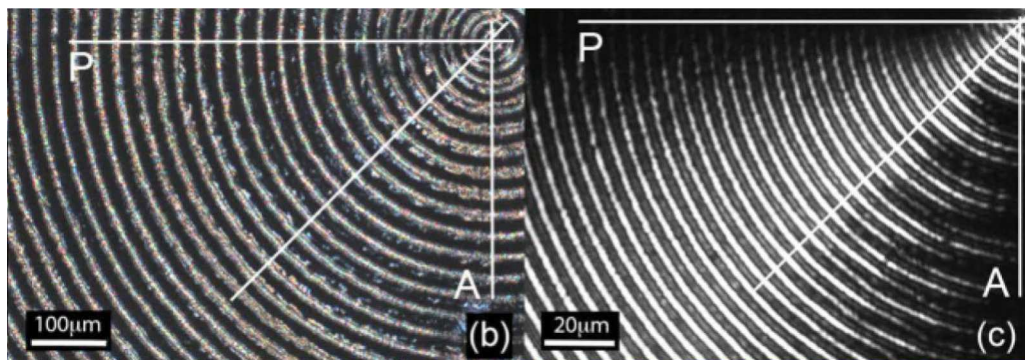


FIGURE 3.3: Micrographs (taken at the POM between crossed polarizers) of the morphologies obtained by exploiting the optical setup

The pictures show how samples look at POM a well defined concentric geometry with bright and dark areas. Indeed, between crossed polarizers, a system with a good radial/circular alignment of the LC director exhibits a very high contrast between the bright areas (around the 45° direction where the maximum of intensity is expected) and the dark ones, which are along

the polarizer and analyzer directions [5]. In Figure 3.3(b) and (c), two angular portions of the samples with smaller pitches are reported. A comparison of the three micrographs shows the best LC alignment in the sample with the smallest pitch ($\Lambda_c \approx 5 \mu\text{m}$). The reason lies in the dynamics of the curing process. According to a previously implemented model [6], a continuous of curing regimes exists, which range from poor to perfect phase separation conditions. In fact, the resulting morphology of the photo-cured structure is affected by the interplay between reactions of polymerization and a mass diffusion process that takes place during curing, and depends, in a quite complex way, on the values assumed by two control parameters: G , related to the curing intensity I , and B , related to the ratio between the diffusion parameter (which depends on temperature T) and Λ . Since in our experiments we have fixed both $T \approx 75^\circ\text{C}$ and $I (\approx 1.2 \text{ mW/cm}^2)$, the only varying parameter is Λ , whose different values determine switching between different curing regimes, that means different realized morphologies. If Λ is small enough, [$\Lambda_c \approx 5 \mu\text{m}$, Figure 3.3(c)], B is quite large, and an almost complete phase separation between polymer and LC components occurs, which produces the best example of polar POLICRYPS structure. By increasing Λ [$\Lambda_b \approx 25 \mu\text{m}$, Figure 3.3(b)], the resulting decrease of B determines a curing condition that crosses the narrow border between POLICRYPS and HPDLC regimes, and the LC component almost completely nucleates in droplets encapsulated in a polymeric matrix. A further smaller B value ($\Lambda_a \approx 100 \mu\text{m}$) corresponds to a regime that probably lies in the POLICRYPS region, but very close to the border with the HPDLC area. Figure 3.2 shows, indeed, a morphology that represents an intermediate result between (b) and (c). Looking at the micrograph along the diagonals, a bright region is observed, which indicates that a given amount of well aligned LC has created a separated phase between two consecutive rings. However, a complete phase separation did not occur and a quite large amount of LC remained trapped in droplets in the polymeric rings, which appear, therefore, differently colored. It is worth noting, however, that once the value of the period Λ has been fixed, the resulting morphology is always the same, turning out to be very reproducible. In particular, the morphology of the grating of interest for optical applications [pitch $\Lambda_c \approx 5 \mu\text{m}$, part (c)] always consists, in all the samples we have fabricated, of rings of pure polymer alternated to rings of pure and well aligned LC. We underline, however, that the typical LC homeotropic alignment between polymer slices, which is the fingerprint of Cartesian POLICRYPS structures, is due to the interaction of polymeric thiolene systems with LC molecules; in

presence of a polar geometry, the same chemical interaction should ensure a radial alignment of the LC director. Where the optical properties of our samples are concerned, they produce a far-field diffraction pattern given by a series of concentric rings. If this pattern is observed at a distance z from the sample, the radius r_m of the m th ring, as deduced from Bragg's formula, is derivable from

$$\Lambda = \frac{m\lambda}{(z/\sqrt{r^2 + z^2}) \tan(\theta_m)} \quad (3.1)$$

where Θ_m is the diffraction angle of the m th order while λ and Λ are the wavelength of the probe beam and the fringe spacing of the circular structure, respectively. The figure 3.4 shows the circular diffraction pattern produced by the sample with $\Lambda_c \approx 5\mu m$, when it is acted on, at normal incidence, by a green laser probe ($\approx 10\mu W$, solid state laser); the screen is put at $z = 1$ m from the sample. Almost equally spaced diffraction rings are located at a distance $r_m = m(5.5)mm \pm 25\%$ from the center, against the predicted value $r_m^{th} = m(5.33)mm$ [Eq.3.1], where the integer m refers to the m th ring. We observe that the intensity of the different diffracted orders decreases by increasing the number of the order. However, as a difference from the Cartesian case, measuring the diffraction efficiency of a given order is now more difficult, the light being diffracted in a ring and no more in a point. An estimate of the first-order diffraction efficiency (performed by means of geometric considerations) has given a value of about 20%.

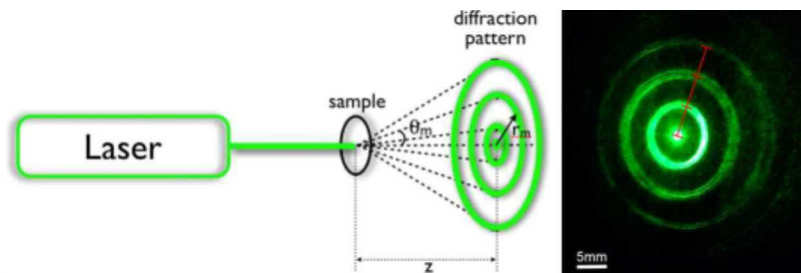


FIGURE 3.4: Sketch of the diffraction pattern produced by a circular diffraction grating when illuminated with coherent light and (right) picture of the diffraction pattern produced by the polar POLICRYPS probed with green laser light

However, both energetic considerations and switching values reported for curved POLICRYPS structures of bigger dimensions [8] bring us to predict

that quite high values are needed to reorient the LC director in our polar POLICRYPS structures. This system allows a simple method for fabricating circular optical diffraction gratings. The produced diffractive pattern is made of concentric bright rings whose radius can be calculated by using Bragg's equation. The technique offers freedom in the choice of the fringe spacing, and values in the range 5 - 100 μm have been achieved. The optical setup for realizing the utilized polar POLICRYPS structures is made of readily available optical elements without need of any custom designed optical items. Modification of distances between optical elements, or their substitution with other ones with different focal length, can allow controlling the number of annular apertures and their periodicity. Morphology of obtained structures largely depends, however, on their pitch; thus, in case a particular application of polar POLICRYPS has to be designed, the best morphological result, for a given pitch, will correspond to a careful choice of all involved curing parameters. Reported results may extend the large range of applications already demonstrated for Cartesian POLICRYPS. Raman analysis to determine the director orientation in LC rings and measurement of light polarization at different positions around the rings of the diffracted pattern is already going on and represents part of an extensive optical and electro-optical characterization of the new structures.

3.3 Conclusion

In this chapter we have reported a novel holographic technique for realizing POLICRYPS composite structures containing LCs organized in a radial alignment. The simple method allows the fabricating of circular optical diffraction gratings. When operated at normal incidence, these structures produce diffractive patterns made of concentric bright rings whose radius can be calculated by using Bragg's equation. The technique offers freedom in the choice of the fringe spacing, and values in the range 5 - 100 μm have been achieved. The optical setup for realizing the utilized polar POLICRYPS structures is made of readily available optical elements without need of any custom designed optical items. Modification of distances between optical elements, or their substitution with other ones with different focal length, can allow controlling the number of annular apertures and their periodicity. Morphology of obtained structures largely depends, however, on their pitch; thus, in case a particular application of polar POLICRYPS has to be designed,

the best morphological result, for a given pitch, will correspond to a careful choice of all involved curing parameters. Reported results may extend the large range of applications already demonstrated for Cartesian POLICRYPS. Raman analysis to determine the director orientation in LC rings and measurement of light polarization at different positions around the rings of the diffracted pattern is already going on and represents part of an extensive optical and electro-optical characterization of the new structures

Bibliography

- [1] Caputo R, De Sio L, Sukhov A V, Veltri A and Umeton C *Opt. Lett.* 29 1261 (2004)
- [2] L. De Sio and C. Umeton, *Opt. Lett.* 35, 2759-2761 (2010).
- [3] M. Infusino, A. Ferraro, A. De Luca, R. Caputo, and C. Umeton, *J. Opt. Soc. Am. B* 29, 3170 (2012).
- [4] D. Alj, R. Caputo, and C. Umeton, *Opt. Lett.* 39, 6201-6204 (2014).
- [5] R. B. Gwynn and D. A. Christensen, *Appl. Opt.* 32, 1210 (1993).
- [6] R. Caputo, L. De Sio, A. V. Sukhov, A. Veltri, and C. Umeton, *Opt. Lett.* 29, 1261 (2004).
- [7] L. De Sio, N. Tabiryan, R. Caputo, A. Veltri, and C. Umeton, *Opt. Express* 16, 7619 (2008).
- [8] A. Veltri, R. Caputo, C. Umeton, and A. V. Sukhov, *Appl. Phys. Lett.* 84, 3492 (2004).
- [9] L. De Sio, N. Tabiryan, and T. Bunning, *Appl. Phys. Lett.* 104, 221112 (2014)

Chapter 4

Polar POLICRYPS and CVB

From

©Appl. Phys. Lett. 107, 201101 (2016)

Part of the work herein reported is reprinted/adapted with permission,
from, D. Alj, S. Paladugu, R. Caputo, G. Volpe and C. Umeton

Polar POLICRYPS diffractive structures generate cylindrical vector beams

4.1 Introduction

As mentioned in the first chapter, a circular symmetry is one of the most common ways used to realize optical devices. When such a symmetry is achieved with birefringent materials like LCs, a special influence on the properties of light can be performed. Particularly interesting is the possibility to control the polarization of a light beam in a good and predictable way. The devices allowing, through the use of birefringent materials, the manipulation of the local state of polarization (SOP) attract every day more interest in Research. For example, a light beam entering a similar device with uniform polarization can exit it with SOP that is spatially variable over the beam area and tunable if the involved materials are reconfigurable. This holds the promise of exploiting novel effects and phenomena that can potentially expand the functionalities and enhance the capabilities of actual optical systems. As introduced in the first chapter, very soon, the appearance of a novel generation of optical devices (4th generation optics) will change the way we imagine functionalities in Optics and Photonics [1]. Great attention is actually devoted to the study of devices able to manipulate a light beam and produce

a cylindrical symmetry of its state of polarization. This is the case of the so-called Cylindrical Vector Beams (CVBs). In recent years a lot of new methods have been reported for CVB generation [2] and they are mainly divided in active and passive methods. What is often in charge to transform the initial polarization (linear/circular) into a new symmetric one, is an element able to influence the polarization in a radial or circular direction. It means that spiral phase elements (SPE), variant $\lambda/2$, Spatial Light Modulator (SLM) or q-plate are excellent candidate for CVB generation. Mathematically speaking, CVBs are vector solutions of Maxwells equations that obey axial symmetry in amplitude, phase and polarization [2, 3]. As shown in Figure 4.1, the simplest 1st-order CVB can be expressed as the superposition of two orthogonally polarized 1st-order Hermite-Gaussian (HG) beam [2]. A radially polarized CVB is obtained as

$$\mathbf{E}_r^{CV}(x, y, z) = HG_{10}(x, y, z)\hat{x} + HG_{01}(x, y, z)\hat{y} \quad (4.1)$$

and an azymuthally polarized CVB as (fig.1b)

$$\mathbf{E}_a^{CV}(x, y, z) = HG_{10}(x, y, z)\hat{x} - HG_{01}(x, y, z)\hat{y} \quad (4.2)$$

Also another 1st-order CVB exists, e.g., a superposition of the radial and azimuthal CVBs leading to the hybrid CVB shown in Fig. 1c. The interest in CVBs arose mainly because of their unique focusing properties due to their polarization symmetry [4, 5]. A radially polarized CVB can be focused into a tighter spot [6, 7] when compared to a Gaussian beam, while the focus of an azimuthally polarized CVB has a donut shape. This has been exploited, e.g., in optical trapping [8], where radial CVBs have been used to trap metallic particles [9, 10] and azimuthal CVBs to trap particles with dielectric constant lower than that of the ambient medium [5]. Switching between radial, azimuthal and hybrid polarization can be done using two half-wave plates [11, 12]. Various alternative methods have been proposed to produce CVBs including: a double-interferometer configuration to convert a linearly polarized laser beam into a radially polarized one [13]; a radial analyzer consisting of a birefringent lens [11]; a surface-emitting semiconductor laser [14]; a space-varying liquid crystal cell [15]; the summation inside a laser resonator of two orthogonally polarized TEM₀₁ modes [16]; the excitation of a few-modes optical fiber with an offset linearly polarized Gaussian beam [17]; a

space-variant dielectric subwavelength grating [18]; a few-modes fiber excited by a Laguerre-Gaussian beam [12]; a conical Brewster prism [19]; and a Sagnac interferometer [20].

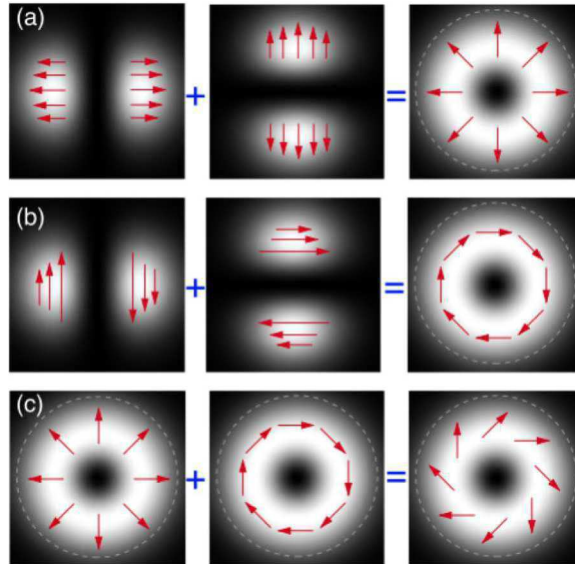


FIGURE 4.1: Cylindrical vector beams (CVBs). (a) Radially and (b) azimuthally polarized 1st-order cylindrical vector beams can be considered as the linear superposition of orthogonally polarized 1st-order Hermite-Gaussian beams. (c) A hybrid CVB can be obtained as the superposition of a radial CVB and an azimuthal CVB. The arrows represent the local direction of the polarization vector.

4.2 Polar POLICRYPS as CVB generator

The polar POLICRYPS structures, considered in Chapter 3, possess some symmetry features in their morphology suggesting a novel way to generate CVBs. A typical polar POLICRYPS (also called polshape) is a polar diffractive structure containing a polymeric support structure and a birefringent material, i.e., liquid crystals (LCs), whose optical axis is radially oriented. This radial symmetry matches the cylindrical symmetry of CVBs and, thus, led us to expect that such polshape could generate a CVB. The fabrication procedure follows the typical POLICRYPS one reported in Chapter 2. The

micrographs of Figure 4.2 show the morphology of the polshape used for the experiments reported in the following.

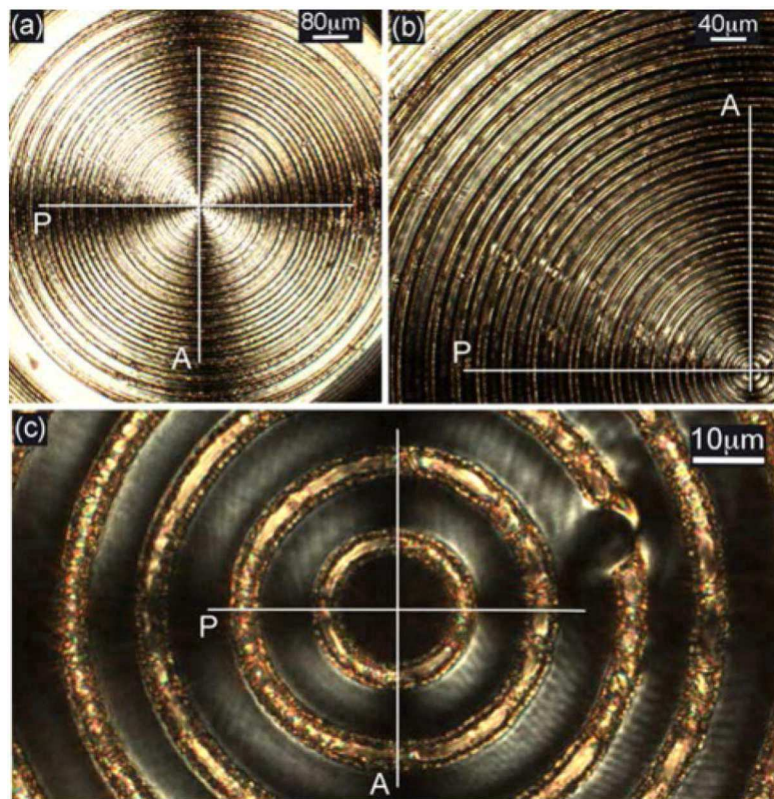


FIGURE 4.2: Micrographs of a POLICRYPS polshape with radial symmetry. All the images are acquired with a polarized optical microscope between crossed polarizers and represent the same sample but at different magnifications. The yellow /light grey rings are the polymeric circles and the dark grey rings are the aligned LC regions.

All images represent the same sample, but at different magnifications, as observed at the polarized optical microscope between crossed polarizers. The Maltese cross confirms the expected radial alignment of the LC molecules between the polymeric rings of the pol shape [26, 27]. Interestingly, the high magnification detail of the center (Figure 4.2c) reveals the contrast between the polymeric circles (yellow/light grey rings) and the aligned (dark grey) LC regions.

The setup used to generate CVBs using the POLICRYPS polshape is centered on the optical path of a He-Ne (633nm) laser beam. The laser beam passes first through a plane polarizer (P) whose axis is parallel to the vertical y-axis and a quarter wave plate (QWP) whose optical axis is kept at $\pm 45^\circ$ with the vertical axis; depending on the sign of this angle, the resulting light beam is

either left circularly polarized (LCP) or right circularly polarized (RCP). Afterwards, the beam undergoes diffraction passing through the characteristic ring structure of the POLICRYPS. Both the diffracted and transmitted beams are then focused onto a CCD camera by a lens. We remark that the part of the beam passing through the polymer rings does not undergo a change of polarization and propagates as a standard TEM₀₀ Gaussian beam because the polymer rings are not birefringent (in fact, while some LC molecules can remain trapped in the polymer, they are not aligned); thus, the beam emerging from the POLICRYPS is a superposition of a pure CVB generated by the LC fringes and the unperturbed (Gaussian) beam coming through the polymer rings. This is a drawback in terms of both the quality of the generated CVB and the efficiency of the device. Nevertheless, the polymeric rings in the structure represents a real valuable advantage since they confine and stabilize the LC material, thus preserving the radial alignment even when the device is used with high-power lasers [26].

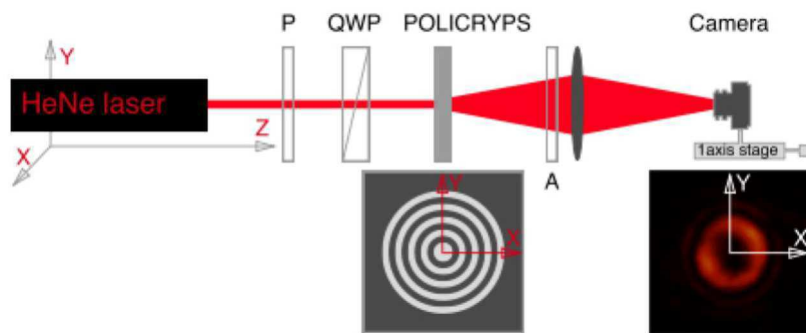


FIGURE 4.3: Setup employed to generate CVBs using the POLICRYPS polshape. It includes a He-Ne laser source (633 nm), a linear polarizer (P), a quarter-wave plate (QWP), a POLICRYPS polshape, a lens, another (removable) polarizer (A), and a camera mounted on a z-axis translation stage.

We illuminated the polshape with a LCP polarized Gaussian beam obtained by adjusting the QWP at 45° with the vertical axis. This generated a diverging CVB, which we could image on a camera by using a lens. Placing the camera at the focal plane of the lens we recorded the beam profile shown in Figure 4.4(a). We then proceeded to measure the components of the beams along various linear polarizations by placing the analyzer before the camera at different angles, i.e., 0° , 45° , 90° and 135° (Figure 4.4b-e, the analyzer axis direction is shown by the white arrow in each panel). We finally used this information to infer the local (i.e., as a function of the coordinates over the

beam profile) Stokes parameters [28, 29] I, Q, U and V , which completely describe the polarization state of a harmonic electromagnetic field. In fact, the polarization ellipse which characterizes a generic harmonic electric field can be written as:

$$I^2 = Q^2 + U^2 + V^2 \quad (4.3)$$

where the Stokes parameters can be expressed in terms of the field components as

$$\begin{cases} I = E_{0x}^2 + E_{0y}^2 \\ Q = E_{0x}^2 - E_{0y}^2 \\ U = 2E_{0x}E_{0y}\cos(\delta) \\ V = 2E_{0x}E_{0y}\sin(\delta) \end{cases} \quad (4.4)$$

where E_{0x} and E_{0y} are the amplitudes of the x- and y-components of the field, and δ is their phase difference. These parameters can be represented as a linear combination of the intensity values measured with the analyzer set at orthogonal polarizations, i.e.,

$$\begin{cases} I = I_0 + I_{90} \\ Q = I_0 - I_{90} \\ U = I_{45} - I_{135} \\ V = I_{RCP} - I_{LCP} \end{cases} \quad (4.5)$$

where I_0, I_{45}, I_{90} and I_{135} represent the measured intensity at each point for linear polarization of the analyzer at $0^\circ, 45^\circ, 90^\circ$ and 135° , respectively, and I_{RCP} and I_{LCP} the intensity obtained using a QWP instead of the analyzer set at -45° and $+45^\circ$, respectively. The polarization angle of the beam is finally given by $1/2 \arctan(U/Q)$ and shown in Figure 4.4(f). The resulting intensity and polarization show a cylindrical symmetry permitting us to identify this beam with a hybrid CVB (Figure 4.1c). This hybrid CVB is the result of the interference between the radially polarized CVB diffracted by the POLICRYPS polshape and the undiffracted illuminating Gaussian beam transmitted through the polshape. Similarly, when we illuminated the POLICRYPS polshape with a RCP Gaussian beam (obtained by adjusting the QWP at $+45^\circ$

with the vertical axis), we generated another hybrid CVB with the same intensity profile, but different polarization.

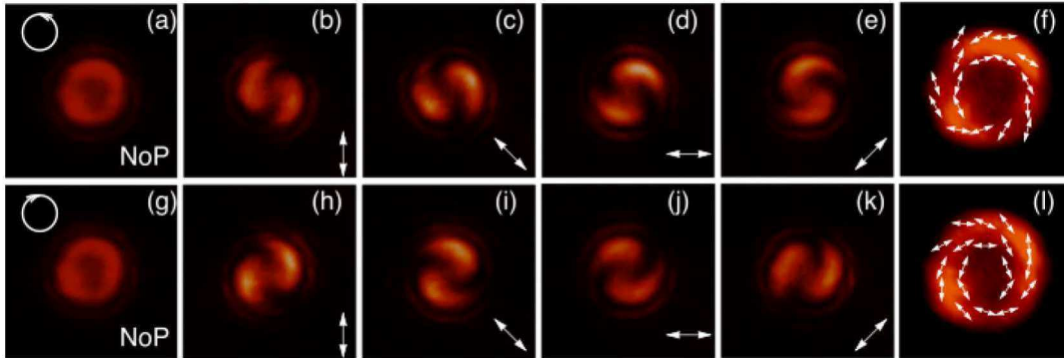


FIGURE 4.4: CVBs generated using a POLICRYPS polshape illuminated with (a)-(f) a LCP Gaussian beam and (g)-(l) a RCP Gaussian beam. (a) and (g) The resulting beams emerging from the polshape, focused by the lens and imaged by the camera. (b)-(e) and (h)-(k) The beams after an analyzer (i.e., a linear polarizer) oriented along the direction of the arrow. (f) and (l) The polarization states measured using Stokes parameters.

shows that the transversal intensity profile of the CVB generated by the POLICRYPS polshape is donutshaped for a quite long path, i.e., at least for ± 10 mm around the focal plane of the lens. This measurement was performed by translating the camera (fixed on a single-axis translation stage) along the z-direction and acquiring transversal images of the beam profile at $10 \mu\text{m}$ steps.

4.3 Conclusion

In this chapter, we have reported the characterization of the behaviour of a polar POLICRYPS structure (polshape) as a cylindrical vector beam generator. What has been realized is a cost-effective device that can locally modify the state of polarization of an incoming beam. This has been achieved by fabricating a birefringent (LC) plate with a specific (radial) orientation of the optical axis. This device allows the conversion of a (left or right) circularly polarized beam into a hybrid CVB. This beam can be further transformed into a pure radial or azimuthal CVB using two half-wave plates [11, 12]. The generated CVB has been experimentally studied by characterizing its polarization and intensity profiles. This study simply represents one of the possible examples of novel active devices that can locally influence the state of

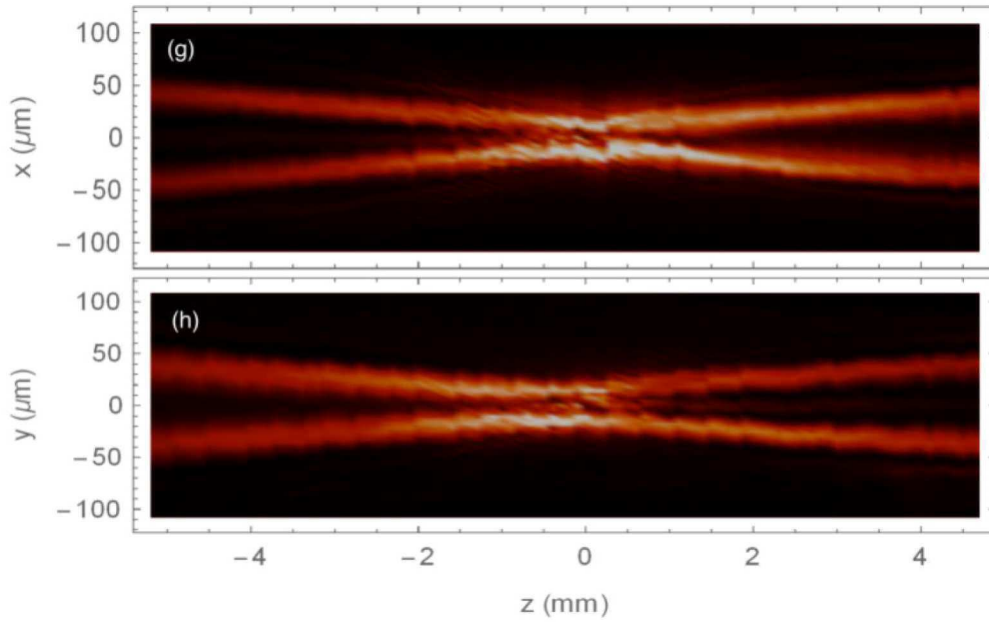


FIGURE 4.5: Transverse beam profiles in the xy -plane at $z=-25$, -15 , -5 , 5 , 15 , and $25 \mu\text{m}$ from the focal plane of the lens.

polarization of a light beam. Moreover, considering that the birefringency of the LC material is electrically tunable, application of an external electric field to the device can turn the POLICRYPS polshape into an active device: the polarization shaping ability of the device can be easily controlled by a knob, up to the point to be modified in real-time or completely switched-off at will.

Bibliography

- [1] N. Tabirian, in 11th Workshop, Novel Optical Materials and Applications (Cetraro, Italy, 2013).
- [2] Q. Zhan, *Adv. Opt. Photonics* 1, 1 (2009).
- [3] D. G. Hall, *Opt. Lett.* 21, 9 (1996).
- [4] Q. Zhan and J. Leger, *Opt. Express* 10, 324 (2002).
- [5] Q. Zhan, *J. Opt. A: Pure Appl. Opt.* 5, 229 (2003).
- [6] S. Quabis, R. Dorn, M. Eberler, O. Gackl, and G. Leuchs, *Opt. Commun.* 179, 1 (2000).
- [7] R. Dorn, S. Quabis, and G. Leuchs, *Phys. Rev. Lett.* 91, 233901 (2003).
- [8] P. H. Jones, O. M. Maragó, and G. Volpe, *Optical Tweezers: Principles and Applications* (Cambridge University Press, 2015).
- [9] Q. Zhan, *Opt. Express* 12, 3377 (2004).
- [10] Q. Zhan, *Proc. SPIE* 5514, 275 (2004).
- [11] Q. Zhan and J. R. Leger, *Appl. Opt.* 41, 4630 (2002).
- [12] G. Volpe and D. Petrov, *Opt. Commun.* 237, 89 (2004).
- [13] S. C. Tidwell, D. H. Ford, and W. D. Kimura, *Appl. Opt.* 29, 2234 (1990).
- [14] T. Erdogan, O. King, G. W. Wicks, D. G. Hall, E. H. Anderson, and M. J. Rooks, *Appl. Phys. Lett.* 60, 1921 (1992).
- [15] M. Stalder and M. Schadt, *Opt. Lett.* 21, 1948 (1996).
- [16] R. Oron, S. Blit, N. Davidson, A. A. Friesem, Z. Bomzon, and E. Hasman, *Appl. Phys. Lett.* 77, 3322 (2000).
- [17] T. Grosjean, D. Courjon, and M. Spajer, *Opt. Commun.* 203, 1 (2002).
- [18] Z. Bomzon, G. Biener, V. Kleiner, and E. Hasman, *Opt. Lett.* 27, 285 (2002).

-
- [19] Y. Kozawa and S. Sato, *Opt. Lett.* 30, 3063 (2005).
- [20] V. G. Niziev, R. S. Chang, and A. V. Nesterov, *Appl. Opt.* 45, 8393 (2006).
- [21] R. Caputo, L. De Sio, A. Veltri, C. Umeton, and A. V. Sukhov, *Opt. Lett.* 29, 1261 (2004).
- [22] M. Infusino, A. Ferraro, A. De Luca, R. Caputo, and C. Umeton, *J. Opt. Soc. Am. B* 29, 3170 (2012).
- [23] L. De Sio, A. Veltri, R. Caputo, A. De Luca, G. Strangi, R. Bartolino, and C. P. Umeton, *Liq. Cryst. Rev.* 1, 2 (2013).
- [24] D. Alj, R. Caputo, and C. Umeton, *Opt. Lett.* 39, 6201 (2014).
- [25] A. Marino, F. Vita, V. Tkachenko, R. Caputo, C. Umeton, A. Veltri, and G. Abbate, *Eur. Phys. J. E* 15, 47 (2004).
- [26] L. D. Sio, N. Tabiryan, R. Caputo, A. Veltri, and C. Umeton, *Opt. Express* 16, 7619 (2008).
- [27] R. Caputo, I. Trebisacce, L. De Sio, and C. Umeton, *Opt. Express* 18, 5776 (2010).
- [28] G. G. Stokes, *Trans. Cambridge Philos. Soc.* 9, 399 (1852).
- [29] M. Born and E. Wolf, *Principles of Optics* (Cambridge University Press, 1988).

Chapter 5

Cellulose Nanocrystals (CNCs)

5.1 summary

- Introduction to CNCs
- CNC Suspension, fingerprint and chiral-nematic phase
- Pitch of the CNC helices and their orientation
- CNCs alignment tests through template molding
- Drying experiments

NOTE: This part has been inspired by the period spent at the University of Luxembourg in the Experimental Soft Matter Physics group.

5.2 Introduction to CNCs

Cellulose Nanocrystals (CNCs) belong to the class of nanomaterials based on renewable resources that are rapidly attracting a growing interest in Chemistry, Physics and Materials Science. Advantages derived from using nature-based nanomaterial are related to ecology sustainability and to the extraordinary performances they can eventually show. Multiple kinds of bioinspired systems for functional materials [1, 2] and Photonics [3] involve many researchers groups in the world. In order to explain the exceptional features of CNCs, it is important to understand their origin. As intuitive from the name, CNCs are derived from cellulose that is one of the most common biopolymer in nature (Figure 5.1). Since its classical use as energy source or paper production, many new technological aspects of cellulose are now studied. If we imagine to check the microscopic structure of wood, we can observe the cellulose cells. They are very different from rod-shaped cellulose nanocrystals.

In particular, the nanorods can be found in small constituents of cellulose cells, called microfibrilles, that can be obtained from the hydrolisis of multiple cellulose-rich resources. Once the microfibrilles are available, by utilizing different procedures, it is then possible to separate these special rods and store them in suspensions. Another kind of CNCs can be synthesized from the particular world of bacteria, they are called bacterial nanocellulose [4, 5, 6, 7, 8, 9]. Extraction of CNCs as reported in literature [4], follows two main steps. In the first step, to achieve uniform reaction conditions, purification and homogenization of the source material is done. Thus, in the second part, the separation of purified cellulose material into its microfibrillar and/or nanocrystalline components is performed. Even following these two steps, the procedure is to be adapted for every cellulose source and the techniques used in each step may employ different solutions (e.g. enzymatic hydrolis instead of mechanical treatment in order to separate microfibrillar or nanocrystalline components [6, 10, 11]

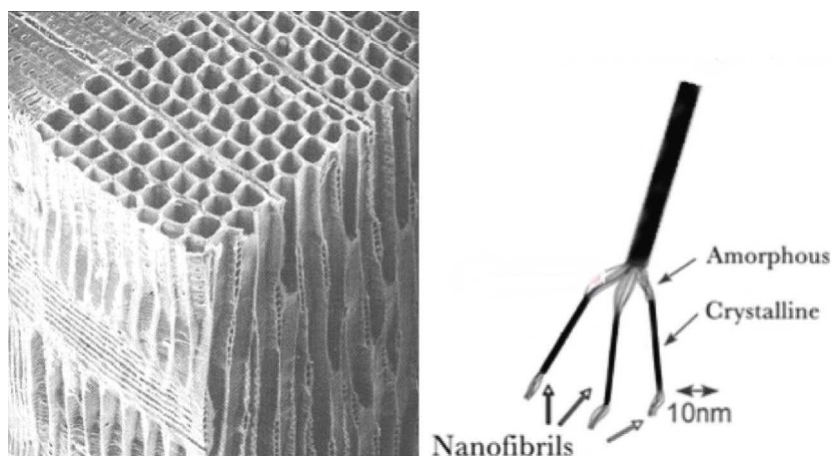


FIGURE 5.1: Cellulose cells (left) and the Nanofibrils (right) from which the CNCs are derived.

5.3 CNC suspension, fingerprint and chiral-nematic phase

Cellulose Nanocrystals are generally stored in suspension, e.g. water suspension in low concentration. From very small concentration (less than 1 wt%) to high concentrated suspensions (ca 15 wt%) their appearance and behavior strongly change. If the concentration of the rods is very small, the

phase in the suspension is isotropic but, as soon as the concentration increases, the phase rapidly changes to nematic and chiral nematic ones that often co-exist. In more detail, by increasing the CNCs concentration, the typical behaviour is that the nematic phase appears first. Then, almost immediately, the alignment director rotates along one axis (Figure 5.3) to reach the typical chiral nematic phase of CNCs. Nematic and chiral nematic states of CNCs show many differences while performing experiments. The most common experiments use to dry the water in suspension in order to observe the final arrangement of the CNCs. In these experiments, the disposition can be studied through the observations that a polarized optical microscope can enhance in a birefringent material. The chiral nematic state is suggested by the typical fingerprint texture that appears after drying (Figure 5.2). As proposed and demonstrated in [12], during drying experiments, the initial concentration of the suspension is a critical parameter that can be fundamental in determining the final disposition of the helices. At the moment, the realization of a large-area uniform helices orientation is one of the most challenging aspects of the research on CNCs.

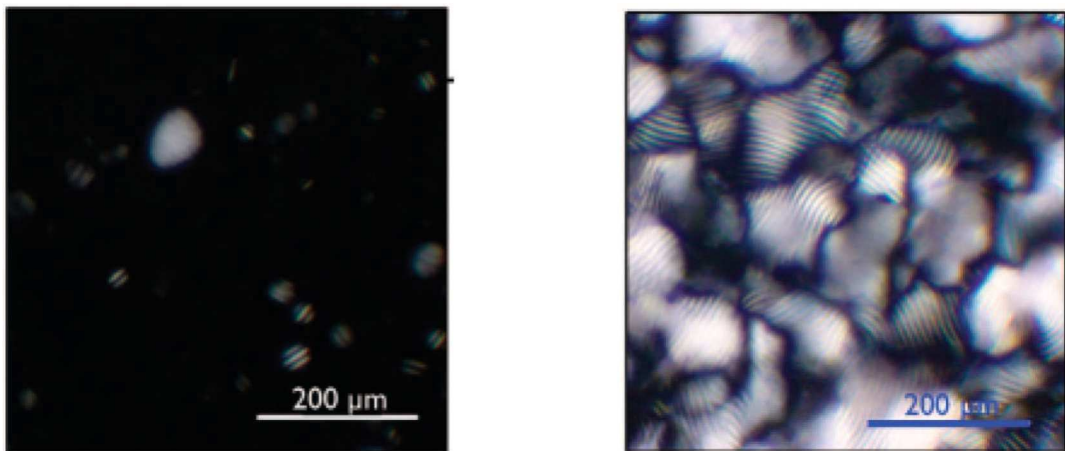


FIGURE 5.2: POM texture from low concentrated suspension (left) where the bright line individuate the liquid crystal fraction in the isotropic (black) material and, (right) fully cholesteric phase. Both from [4]

5.4 Pitch of the CNC helices and their orientation

When the concentration is large enough for determining the chiral-nematic phase, the resulting helical pitch value in CNCs suspensions is typically around

10 μm or more. This is way too far from the characteristic size of a typical optical device that efficiently interacts with light in the visible range (400 to 700 nm). However, even if the measurement of the helical pitch in suspension has already been demonstrated [13, 14], CNCs drying experiments almost always result in an optical behavior whose features are visible by naked eye. This apparently contradictory phenomenon has raised the researchers interest who are, since then, strongly involved in intensive discussions and thorough investigations to clarify it. The recent review works found in literature [4, 12], describe how the features of CNCs change and influence the possible results in drying experiments. In case of very low CNCs concentration, in some areas of the sample, the helices can self-dispose with their axes parallel to the substrate. This kind of alignment is demonstrated by POM observations showing textures characterized by widely spaced parallel lines. In this case, the CNCs material thickness is very thin and mainly a layer of parallel aligned helices is expected (no bulk material). As suggested in [4], the parallel disposition can also appear during the drying of highly concentrated solutions, due to the interaction of a superficial layer of CNCs with the air interface. This time, being the parallel disposition of helices only present in the upper part of the sample surface, it may happen that the disposition in the bulk is vertical and thus can be indirectly observed by selective colors reflections. Finally, for getting a more uniform disposition of helices of CNCs, better results can be achieved in presence of a fully liquid crystalline suspension at the beginning of experiments. For achieving this condition, a concentration around 10 wt% of CNCs in water is necessary [15]. When the aimed outcomes of this kind of research are concerned, the best case of drying experiments is the achievement of a uniform distribution of helices of CNCs in vertical disposition and on large-area sample substrates. In ver-



FIGURE 5.3: Helix sketch. From [4]

tical disposition, the CNCs helices show peculiar optical properties due to the related intrinsic chirality of the structures. In general feature, the optical properties of chiral (cholesteric) liquid crystalline materials are well known from long time [16, 17]. In particular, the reflected light emerging from chiral structures shows a specific circular polarization. In detail, the handedness of the emerging circular polarization depends on the handedness of the chiral structures as well as on their pitch [16]. This considered, an fundamental question about the optical interaction shown by light and CNCs helical structures stands out: if, as already mentioned, the helical pitch in suspension ($\approx 10 \mu m$) is not comparable with the visible wavelength, how it comes that the interaction of light with a dried film of CNCs is well visible also by naked eyes. In this sense, on the basis of the various observations, a reliable possibility is that the evaporation of water promotes the helical collapse from 10 to $0.3 \mu m$. Moreover, a possibly not perfect vertical alignment of the helices but a distribution of orientations takes place during the drying process because experimental proofs also show, for the reflected light, a predictable dispersion and different wavelengths (Figure 5.4) are reflected depending on both the helix angle with the substrate and the viewing angle.

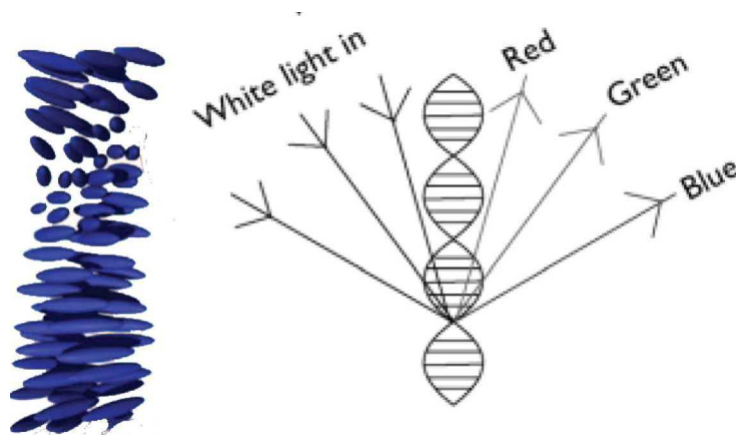


FIGURE 5.4: Helices sketch (from [4]) (a), Reflection from an helix (b).

5.5 CNCs alignment tests through template molding

Several techniques have been considered for aligning CNCs. Among them, drop casting (circular symmetry) and shear flow (broken symmetry) experiments have been performed in different ways by varying concentration and kind of CNCs. In these experiments, an iridescent sequence of colors can be obtained as a result of the evaporation. In case of a drop-casting experiment, due to the symmetry of the CNCs suspension droplet, the evaporation produces a distribution of the material that changes in annular regions (visible in the resulting iridescent film). Indeed, it is possible to distinguish these annular regions for their same colour and this is a hint of an almost uniform disposition of helical structures. A long description of dried CNC films is again discussed in [4] where more solutions have been proposed about the phenomena intervening during the drying of CNC droplets. Special attention is given to all the effects promoting or influencing the vertical disposition on the sample surface. Multiple parameters influence the final results and, for this reason many efforts in research are focused to characterize other aspects of the large family of CNCs (e.g.[18]). In this work, it has been considered an alternative possibility to influence the disposition of CNCs during drop casting experiments. Some preliminary tests have been done by using POLICRYPS templates as molds (Figure 5.5). As an attempt, the mold was on one of the two glass substrates of an opened circular POLICRYPS cell where the LCs have been almost completely washed away by using a solvent (tetrahydrofuran)[19, 20]. This preliminary test followed the classical procedure of a drop casting experiment:

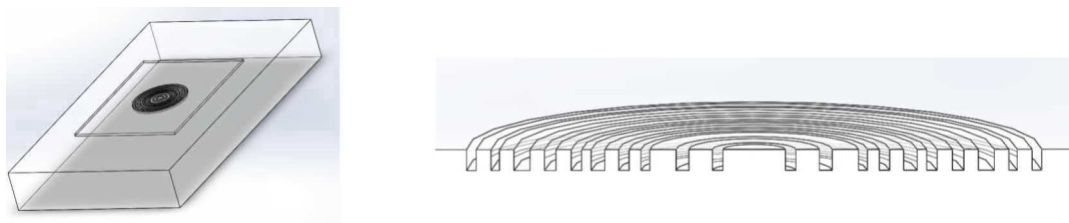


FIGURE 5.5: Sketches of template replica, realized in PDMS, section on the right

- First, a PDMS template where the POLICRYPS mold has been replicated is exposed to a plasma treatment in order to become hydrophilic.

This is an important requirement to assure the perfect wettability of the substrate by the CNCs suspension;

- CNCs suspension is deposited with a micropipette. In this step, the size of the droplet can determine the final result;
- the drop is left to dry. In some experiments the environment has been controlled with the employment of humidity and temperature controller (not in this case). This can get more chances to dry the suspension in a desired way in order to reach a more ordered film of CNCs.

The last step may require long time until the complete evaporation of water (e.g. 20 hours) takes place. Results of these tests are not extremely impressive because the influence of the structures during evaporation has not been particularly effective (Figure 5.6). This does not exactly mean that it is not possible to influence the disposition of CNCs by means of a template structure but there are probably a lot of other parameters to be considered. As well discussed in the works in literature and summarized above, the disposition of CNCs and the achievable chiral structure is a complex ensemble of several parameters. Further works may be focused in using different template symmetries, or different functionalization of the surface. An influencing parameter could be, for instance, represented by the pitch of the structures or the material in which the template is realized.

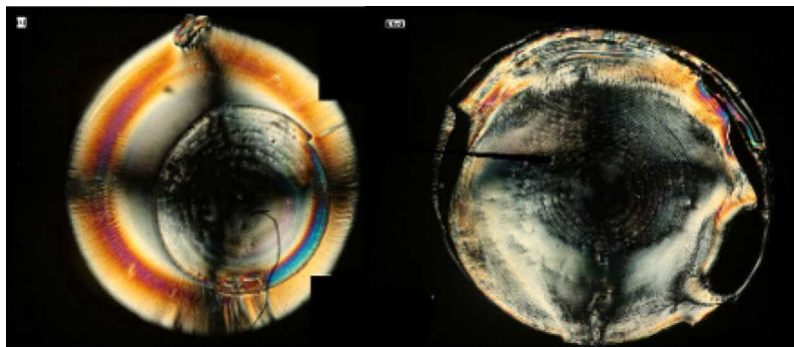


FIGURE 5.6: Molds with dried CNCs suspension on top. Viewing at POM in transmission mode

5.6 Drying experiments

Following the results of multiple drying experiments performed and discussed by scientists, another attempt has been tried. In this case, instead

of a mold replica of a template, a simple empty circular sink of PDMS was realized. The sink was circular with a diameter of 1 cm and a depth of about 0.5 mm.

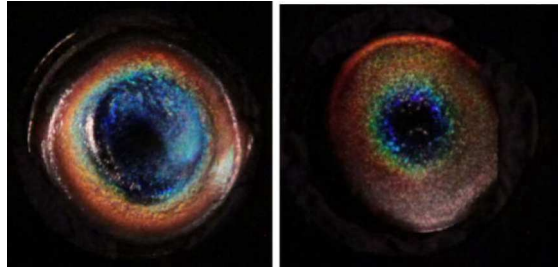


FIGURE 5.7: Two example of drying test performed (diameter 1cm)

A circular cover glass of 1cm diameter has been functionalized and put into the sink of PDMS. The idea is to allow the CNCs suspension to interact with two parts of the sample, one functionalized with plasma treatment and the boundary of the sink, where the surface was not functionalized. The effect of the hydrophobic (PDMS) boundary, allows to put on the circular glass a large amount of CNCs suspension. This required more than one day of drying time in the environment of the lab to obtain the complete evaporation of water and the appearance of iridescent CNC patterns. The results (Figure 5.7) in this case do not look much different from the drying experiments on simple glass substrate Figure 5.8 where a better circular symmetry is evident and a large uniform area is visible.

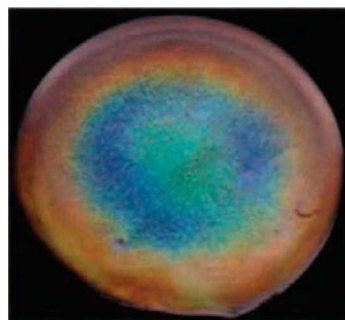


FIGURE 5.8: A sample of CNC with a diameter of 25 mm dried on glass (from [4])

5.7 Conclusions

In this chapter CNCs have been reported as promising materials for applications thanks to their special features. The problems still related with their disposition control during drying experiments are also reported. The experiments performed have shown the problems that occur during experiments.

Bibliography

- [1] Fratzl, P. Biomimetic materials research: what can we really learn from nature's structural materials *J. R. Soc. Interface* 4, 637642 (2007).
- [2] Wicklein, B. & Salazar-Alvarez, G. Functional hybrids based on biogenic nanofibrils and inorganic nanomaterials. *J. Mater. Chem. A* 1, 54695478 (2013).
- [3] Viktoria Greanya PhD, *Bioinspired Photonics, Optical Structures and Systems Inspired by Nature*
- [4] J. P. F. Lagerwall, C. Schtz, M. Salajkova, J. Noh, J. H. Park, G. Scalia, L. Bergström, *NPG Asia Mater.* 2014, 6, e80.
- [5] Klemm, D., Kramer, F., Moritz, S., Lindstrom, T., Ankerfors, M., Gray, D. & Dorris, A. Nanocelluloses: a new family of nature-based materials. *Angew. Chem. Int. Edit.* 50, 54385466 (2011).
- [6] Habibi, Y., Lucia, L. & Rojas, O. J. Cellulose nanocrystals: chemistry, self-assembly, and applications. *Chem. Rev.* 110, 34793500 (2010).
- [7] Moon, R. J., Martini, A., Nairn, J., Simonsen, J. & Youngblood, J. Cellulose nanomaterials review: structure, properties and nanocomposites. *Chem. Soc. Rev.* 40, 39413994 (2011).
- [8] Eichhorn, S. J., Dufresne, A., Aranguren, M., Marcovich, N. E., Capadona, J. R., Rowan, S. J., Weder, C., Thielemans, W., Roman, M., Renneckar, S., Gindl, W., Veigel, S., Keckes, J., Yano, H., Abe, K., Nogi, M., Nakagaito, A. N., Mangalam, A., Simonsen, J., Benight, A. S., Bismarck, A., Berglund, L. A. & Peijs, T. Review: current international research into cellulose nanofibres and nanocomposites. *J. Mater. Sci.* 45, 133 (2010).
- [9] Isogai, A., Saito, T. & Fukuzumi, H. TEMPO-oxidized cellulose nanofibers. *Nanoscale* 3, 7185 (2011).
- [10] Hubbe, M. A., Rojas, O. J., Lucia, L. A. & Sain, M. Cellulosic nanocomposites: a review. *BioResources* 3, 929980 (2008).

- [11] Siro', I. & Plackett, D. Microfibrillated cellulose and new nanocomposite materials: a review. *Cellulose* 17, 459494 (2010).
- [12] Park, J. H., Noh, J., Schütz, C., Salazar-Alvarez, G., Scalia, G., Bergström, L. and Lagerwall, J. P. F. (2014), Macroscopic Control of Helix Orientation in Films Dried from Cholesteric Liquid-Crystalline Cellulose Nanocrystal Suspensions. *ChemPhysChem*, 15: 14771484. doi:10.1002/cphc.201400062
- [13] Majoinen, J., Kontturi, E., Ikkala, O. & Gray, D. G. SEM imaging of chiral nematic films cast from cellulose nanocrystal suspensions. *Cellulose* 19, 15991605 (2012).
- [14] Beck, S., Bouchard, J., Chauve, G. & Berry, R. Controlled production of patterns in iridescent solid films of cellulose nanocrystals. *Cellulose* 20, 14011411 (2013).
- [15] E. E. Ureña-Benavides, G. Ao, V. A. Davis, C. L. Kitchens, *Macromolecules* 2011, 44, 8990.
- [16] Gray, D.G. Recent Advances in Chiral Nematic Structure and Iridescent Color of Cellulose Nanocrystal Films. *Nanomaterials* 2016, 6, 213
- [17] De Vries, H. Rotatory Power and other Optical Properties of Certain Liquid Crystals. *Acta Crystallogr.* 1951, 4, 219226.
- [18] Honorato-Rios, C.; Kuhnhold, A.; Bruckner, J.; Dannert, R.; Schilling, T.; Lagerwall, J.P.F. Equilibrium Liquid Crystal Phase Diagrams and Detection of Kinetic Arrest in Cellulose Nanocrystal Suspensions. *Front. Mater.* 2016, 3, 75.
- [19] L. De Sio, S. Ferjani, G. Strangi, C. Umeton and R. Bartolino, *Soft Matter* 7 (8), 3739-3743 (2011).
- [20] L. De Sio, P. D'Aquila, E. Brunelli, G. Strangi, D. Bellizzi, G. Passarino, C. Umeton and R. Bartolino, *Langmuir*, 2013, Vol. 29, n. 10, pp. 3398-3403.

Appendix A

Recording Policryps Structures in photonic crystal fiber

From

Part of this appendix is reprinted/adapted from a submitted paper on Photonic Letters of Poland (2017)

D. Poudereux, M. Caño-García, D. Alj, R. Caputo, C. Umeton, M.A. Geday, J.M. Otón and X. Quintana

A.1 introduction

From the original idea of D. Poudereux, a grating made with the POLICRYPS technique has been recorded into a Photonic Crystal Fiber (PCF). The PCF are a special kind of optical fiber where a number of holes is organized in the core of the fiber. These holes modify the effective refractive index of the fiber core and cladding, being effectively responsible of the peculiar guiding properties of PCFs. Filling the holes either all of them or a specific set with any material may have dramatic effects on the PCF waveguide modal distribution [1, 2]. If the filling material is electrooptically active, then tunable devices driven by external signals can be implemented. The infiltration of photonic crystal fibers with liquid crystals has greatly evolved since the first infiltration experiments [3]. The combination of the passive properties of PCFs and the active optical properties of LCs resulted in a new kind of versatile devices, the photonic liquid crystal fibers (PLCF). PLCFs have been developed and manufactured for many applications including optical communications, signal treatment, interferometers and sensors [4, 5, 6, 7].

A.2 Methodology

In the performed experiments two different PCFs (Blaze Photonics) have been chosen for infiltration with POLICRYPS mixture before curing, both having internal holes of two different diameters. The first one is the polarization maintaining photonic crystal fiber PM-1550-01, which has a solid core with two $4.5 \mu\text{m}$ holes at either side of the fiber axis, and a cladding with five rings of $2.2 \mu\text{m}$ holes. The cladding pitch between holes is $4.4 \mu\text{m}$ Figure A.1(left). The second fiber is a hollow core photonic crystal fiber HC-1550-01 with a core diameter of $10 \mu\text{m}$ and a cladding pitch of $3.8 \mu\text{m}$ (Figure A.1(right)).

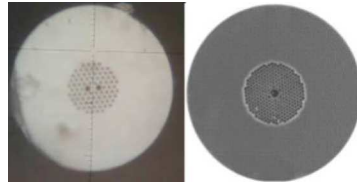


FIGURE A.1: Left PM-1550-01, Right HC-1550.

A selective filling of the holes of the fibers have been done collapsing the smaller hole by using a fusion splicer. In this way long fiber lengths have been collapsed (over 1cm). In this region, only the central large hole/s of the fibers have been filled inside a vacuum chamber. An alternative way is to fill only the smaller holes. To do that, the PCF is filled with a photocurable adhesive (e.g. NOA 61). The different speed in filling by capillarity of the small and large holes, allow to observe under microscope the difference in the filling path.

Then, when the adhesive is cured, the fibers have been cut in the middle of the difference of the filling path. In this way the cured adhesive on the central hole became a “cork” and it is possible to fill with the POLICRYPS mixture, only the small holes.

A.3 results

POLICRYPS recording has been demonstrated in both cases (collapsed cladding and empty cladding). The expected Bragg reflection has not been observed due to the large pitch of the grating ($2\mu\text{m}$). In future works, with a shorter

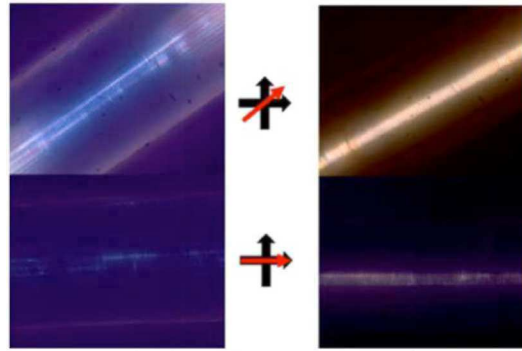


FIGURE A.2: Left: Microphotograph between crossed polarizers of the collapsed region of a PM-1550-01 fiber with a Polycryps recorded in its wider holes, at 45° (top) and parallel (bottom) to the input polarizer. Right: Same arrangement employing HC-1550 fiber; the cladding is collapsed and a Polycryps recorded in the hollow fiber core

pitch of the structures ($0.5 \mu m$) in combination with electrooptical activity of the LCs it is estimated to be observed a tunability range above $50 nm$ in the $1550nm$ region.

Bibliography

- [1] Liu, Q. et al. Tunable Fiber Polarization Filter by Filling Different Index Liquids and Gold Wire Into Photonic Crystal Fiber, *J. Lightwave Technol.* 34(10), 2484-2490 (2016).
- [2] Velázquez-Ibarra, L., Díez, A., Silvestre, E. and Andrés, M.V., Wideband tuning of four-wave mixing in solid-core liquid-filled photonic crystal fibers, *Opt. Lett.* 41(11), 2600-2603 (2016).
- [3] Larsen, T., Bjarklev, A., Hermann, D. and Broeng, J., Optical devices based on liquid crystal photonic bandgap fibres, *Opt. Express* 11(20), 25892596 (2003).
- [4] Choi, H. Y., Kim, M. J. and Lee, B. H., All-fiber Mach-Zehnder type interferometers formed in photonic crystal fiber, *Opt. Express* 15(9), 57115720 (2007).
- [5] Poudereux, D., Corredera, P., Otón, E., Otón, J. M. and Arregui, X. Q., Photonic liquid crystal fiber intermodal interferometer, *Opt. Pura Apl.* 46(4), 321325 (2013).
- [6] Woliński, T. R. et al. Tunable Optofluidic Polymer Photonic Liquid Crystal Fibers, *Mol. Cryst. Liq. Cryst.*, 619(1), 2-11 (2015).
- [7] Budaszewski, D., Woliński, T.R., Geday, M.A. and Otón, J.M., Photonic Crystal Fibers infiltrated with Ferroelectric Liquid Crystals, *Phot. Lett. Poland*, 2(3), 110-112 (2010).

Conclusions

What here has been exposed, is a dissertation about the major activity performed during the the last three years. As it is clear from what has been reported, most part of the activity have been inspired by the POLICRYPS technique because this technique started from the group where the Ph.D course has been spent. The possible applications of POLICRYPS have been demonstrated from the first years of 21th century. The experience in this field need to be strongly related with a good know-how in Liquid Crystals and photopolymerizable mixtures in combination with a good motivation during experiments. From this basis, a novel approach and studies have been performed on gratings using a circular symmetry. First, the main features of a circular grating made by exploiting the POLICRYPS technique has been discussed and detailed in a published work. About this work a lot of discussion is still active about the physics behind the circular pattern generation and research in the direction of a complete numerical characterization of the utilized optical system is ongoing (not reported in this work). Even if the main aspects are clear and related with a self-interference that affects a laser beam in an optical system with an enhanced spherical aberration, a numerical simulation revealed several issues and did not clarify yet how to control and properly customize the circular curing pattern. Further efforts may be then required in the future to realize simulation experiment where a good system has been indicated in ray-tracing simulation. Then, the research has been motivated by the applications that a POLICRYPS circular grating can reach. In more detail, the cylindrical vector beam (CVB) generation has been discussed and demonstrated with a published work. In this work the use of Polar POLICRYPS systems has shown how the morphology of the samples can modify the state of polarization of an incoming beam in order to realize a cylindrical symmetry of the polarization state of the outcoming beam. Even if the generated CVB has been seen as a superposition of two effects (a well modified polarization as CVB and a not re-arranged ones due to the presence of polymeric walls), these experiments demonstrate the possibility to realize a cost-effective device. The direction where the novel studies can be oriented are related with the electric tunability allowed by LCs. These can transform the polar POLICRYPS into an active device, completely switchable, with interesting practical applications. This work has been realized in collaboration with the group of Prof. Giovanni Volpe at Bilkent University. The interest in materials and technique that allow, especially for their symmetry, an optical application has also interested the novel field of Cellulose Nanocrystals. Their features as optical ma-

materials in combination with their eco sustainability as biomaterials are an intense field of research. In this sense, the big challenges that surrounds these materials (orientation, control of their self-assemble process) have represented a good motivation to make some experimental attempt. This has been possible thank to the collaboration with the group of Prof. Ian Lagerwall at the University of Luxembourg. The proposed experiments were related with the influence that a replica in PDMS of a POLICRYPS template would be able to induce on a CNCs suspension during a drying experiment. Results on this sense have not been very impressive but have suggested some hints for further tests.